R-99-44

SR 97 – Alternative models project

Channel network modelling of Aberg

Performance assessment using CHAN3D

Björn Gylling
Kemakta AB

Luis Moreno, Ivars Neretnieks
Department of Chemical Engineering
and Technology, KTH

June 1999

Svensk Kärnbränslehantering AB
Swedish Nuclear Fuel
and Waste Management Co
Box 5864
SE-102 40 Stockholm Sweden
Tel 08-459 84 00
+46 8 459 84 00
Fax 08-661 57 19
+46 8 661 57 19

ISSN 1402-3091
SKB Rapport R-99-44

SR 97 -
Alternative models project

Channel network modelling of Aberg

Performance assessment using CHAN3D

Björn Gylling
Kemakta AB

Luis Moreno, Ivars Neretnieks
Department of Chemical Engineering
and Technology, KTH

June 1999

Keywords: Performance Assessment, Radionuclide Transport, Pathways Analysis, Fracture Flow, Near-Field, Far-Field, FARF31, COMP23, FracMan, PA Works.

TABLE OF CONTENTS

1 INTRODUCTION

In Sweden and in many other countries, spent nuclear fuel storage at depth in crystalline rock is planned. Repository conditions typically involve low water flow rates and long distances. In the performance assessment of a repository, modelling of water flow and solute transport is an important task. In earlier papers (Moreno et al. 1997; Gylling et al. 1998a), discussions of the mechanisms which are important in performance assessment in fractured media are given. The influence of the mechanisms has been demonstrated using CHAN3D. The main objectives of these studies were to highlight the important transport mechanisms, to present the Channel Network model and to show the capabilities of the tool. In one of these exercises (Gylling et al. 1998a), NUCTRAN - COMP23 (Romero et al. 1995a-b) was integrated into CHAN3D as a temporal source term for radionuclides. In the present study, CHAN3D is used to calculate input entities to COMP23 and the far field code FARF31.

2 OBJECTIVES AND BACKGROUND

One of the activities in the SR 97 project is to demonstrate the barrier performance of the rock using different alternative models for flow and transport (Ström and Selroos, 1997). In this report, the use of the CHAN3D concept for performance assessment is described. The results may later be used for comparison with the ones obtained by groups using other concepts, such as HYDRASTAR and FRACMAN.

The objectives for this part of the project are:

- To illustrate the rock barrier performance using different conceptual models for groundwater flow and mass transport in fractured rock.
- To show how robust the assessment model description is in terms of relevant far field performance measures.

2.1 Task definition

In the first step, the model is used for providing the near field model COMP23 and the stream tube far field transport code FARF31 with input parameters. The stream tube concept imposes restrictions on the method of obtaining these model parameters. Examples of these restrictions are simplified near field flow pattern and the use of pre-determined transport dispersion.

Spatially constant porosity and flow-wetted surface, FWS, are adopted in the main hydraulic analysis (using HYDRASTAR) within SR 97. However, spatially varying properties were used in the CHAN3D simulations, which were used to the developed features of the concept. In the CHAN3D calculations performed for this task, an experimentally determined value for the specific flow-wetted surface in the fracture zones was used. This part of the project is bounded by the following conditions:

- The first step is limited to data from Aberg, i.e. the Äspö site. Use of data from Sicada was emphasised.
- Each group should describe their data evaluation process or model parameter abstraction process in a common format.
- The study is limited to three repository blocks at the 500 m level.
- A number of canister locations is determined.
- Modelling domain and boundary conditions should be consistent with the study performed by Svensson, (1997).
- Fresh-water head values from the regional Phoenix calculations performed by Svensson (1997) is used as boundary conditions.

The obtained input entities to FARF31 and COMP23 are:

- q, Darcy velocity, at canister scale
- a_w, FWS per volume of water representing complete path
- t_w, groundwater travel time
- Pe = qL/D, Peclet number

2.2 Output entities

Since the project specification includes the Peclet number assumed by Andersson et al. (1998), we have omitted Pe in our calculations. The output entities for the paths, i, in each realisation, k, are:

- Distribution of q_i for all canisters
- Distribution of travel times, t_i, for all canisters
- Distribution of F-ratio for all paths, defined as $F_i = \sum t_i \cdot a_{w,i}$
- Distribution of $a_{w,i}$ for all the paths

Since the variability in the entities, denoted by x, may be large it was decided that the entities should be calculated in $\log_{10}$-space, denoted y where $y = \log_{10}(x)$.

In the simulation process, every single entity result is recorded for use in the ensemble statistics. The number of values used in the ensemble statistics is equal to the number of realisations times the number of path lines in each realisation. For the ensemble statistics, mean, variance, median, 5^{th} and 95^{th} percentiles and a measurement of dispersion (defined as $D_y = y_{95\%} - y_{5\%}$) are documented. Results and histograms from two typical realisations and three specified canister positions are also reported. Path line exit locations are studied in the realisations.

In addition, statistical moments (mean and variance) and other statistical measurements of the output entities; q_i, t_i, F_i and $a_{w,i}$ are calculated in each realisation for use in the performance measure calculations. The notation $\bar{y}$ and σ^2_y are used for the moments (mean and variance) and y_{50} is used for the realisation median.

2.3 Performance measures

Performance measures, i.e., averaging over the ensemble of all realisations are also calculated. Statistical estimates of the entities mentioned above defined as mean ($\bar{y}$) and variance, VAR[$\bar{y}$], are reported in addition to median and spread of realisation median values, y_{50}. Variations can be expressed using the mean of σ^2_y and the variance of σ^2_y. Performance measures may be also expressed as the median of the dispersion in results, MD_y and the spread in D_y defined as $UD_y = (D_y)_{95\%} - (D_y)_{5\%}$.

The performance measures are defined as statistical estimates of the entities mentioned above i.e. mean and variance of the Darcy-velocity, q_k, of groundwater travel time, t_k, of the F-factor and of the specific flow-wetted surface, a_w. Results representing all realisations are presented in this study. Based on the results, some canister positions are selected and evaluated in more detail.

In summary, the following performance measures are calculated in this report:

- Moments (mean and variance) of $\bar{y}$ and σ^2_y
- Median, percentiles, dispersion and histograms of y_{50}

3 APPLICATION OF THE MODEL TO THE SITE ABERG

3.1 Simulation domain and boundary conditions

The same simulation domain as in Svensson, (1997) is used. The coordinates defining the domain are shown in Table 1. This means that the simulation volume is 4 km^3. The coordinate system is right hand oriented with positive X towards east.

Table 1. Äspö coordinates of the domain.

Coordinate	Positive direction	Minimum	Maximum
X	Eastward	1 000	3 000
Y	Northward	6 000	8 000
Z	Up	-1 000	0

It has been decided that the fresh-water head boundary condition from the calculations by Svensson, (1997) should be used. The topography was explicitly taken into account in the regional study, which used different types of boundary conditions depending on the areas covered, by land and by sea. Fresh-water head and Darcy flux values have been delivered for top, bottom, northern, southern, eastern and western sides. The flux values are obtained for a 100 m x 100 m area.

3.2 Fracture zones and delimiting planes

The major fracture zones at the Äspö site are described in Rhén et al. (1997). Eighteen of them fall within the modelling domain. The fracture zones are shown in Figure 1. All the zones start at the surface (Z = 0) and continue to the bottom of the simulation domain except NNW-8, which

does not exist over Z = -300 m and below Z = -700 m. The transmissivity values, T, have been obtained from hydraulic borehole tests except for zone SFZ14 where the T-value is estimated. In addition to the fracture zones, other areas have been found to have properties different from those of the rock mass. These site-scale rock domains are called SRD and are characterised by anomalous rock mass conductivity due to high fracture frequency, different rock types or both. Table 2 shows the fracture zones in the modelled rock volume, the planes delimiting these zones and the fracture-zone transmissivity. Planes BW01-BW04 correspond to the lateral boundaries of the model (eastern, southern, western and northern respectively). The other planes (A:s, F:s and Q:s) are used to define specific fracture zones.

Table 2. Fracture zones in the modelled rock volume for Aberg.

Zone name	Planes defining the zone	Transmissivity (median), [m^2/s]
EW-1N	BW03, BW04	1.5E-06
EW-1S	BW01, BW03, BW04	2.2E-05
EW-3	NE-1, BW03	2.4E-05
EW-7	NE-4N, BW01	6.8E-05
NE-1	BW03, BW01	3.0E-04
NE-2	EW-1S, NE-1, EW-3	4.1E-07
NE-3	BW01, BW02, BW03	2.9E-04
NE-4N	BW01, BW03	3.0E-05
NE-4S	NE-4N, BW02	3.0E-05
NW-1	EW-1N, BW04	1.7E-07
NNW-1	EW-3, EW-1S	1.1E-05
NNW-2	NE-1, EW-1S	5.6E-05
NNW-3	F2, F3	2.0E-05
NNW-4	NE-1, EW-1S	1.5E-04
NNW-5	NE-4N, F1	2.0E-06
NNW-6	EW-7, NE-4N, NE-1	1.4E-05
NNW-7	EW-3, EW-1S	4.8E-06
NNW-8	EW-1N, A1, A2, BW04	1.0E-05
SFZ11	NE-1, BW01	1.0E-04
SFZ14a	BW03, SFZ14b	1.0E-04
SFZ14b	SFZ14a, BW04	1.0E-04

3.3 Repository layout

The canisters containing the spent fuel are located at a depth of 500 m. In this modelling exercise the block units 3, 4, and 6 in the proposed layout by Sandstedt et al. (1997) will be used. In total, there are 945 canisters and 11 tunnels in these three blocks. The tunnels in each block are shown in Table 3 together with their lengths. The dimensions for the deposition tunnels and the canisters are shown in Table 4. The canisters are located at the bottom of the tunnels and are separated by a distance of 6 m. The fracture zones together with some of the tunnels are shown in Figure 1.

Table 3. Tunnel layout and tunnel lengths.

Block unit	Tunnel ID	Length	Number of canisters
3	9	393	66
3	10	581	97
3	11	628	105
3	12	675	112
3	13	722	120
4	14	492	82
4	15	445	74
4	16	398	66
4	17	351	59
4	18	231	38
6	21	757	125

Table 4. Dimensions of tunnels and deposition holes (Sandstedt et al. 1997).

	Height	Width
	[m]	[m]
Tunnel	4.0	3.6
Deposition hole	7.833	1.75

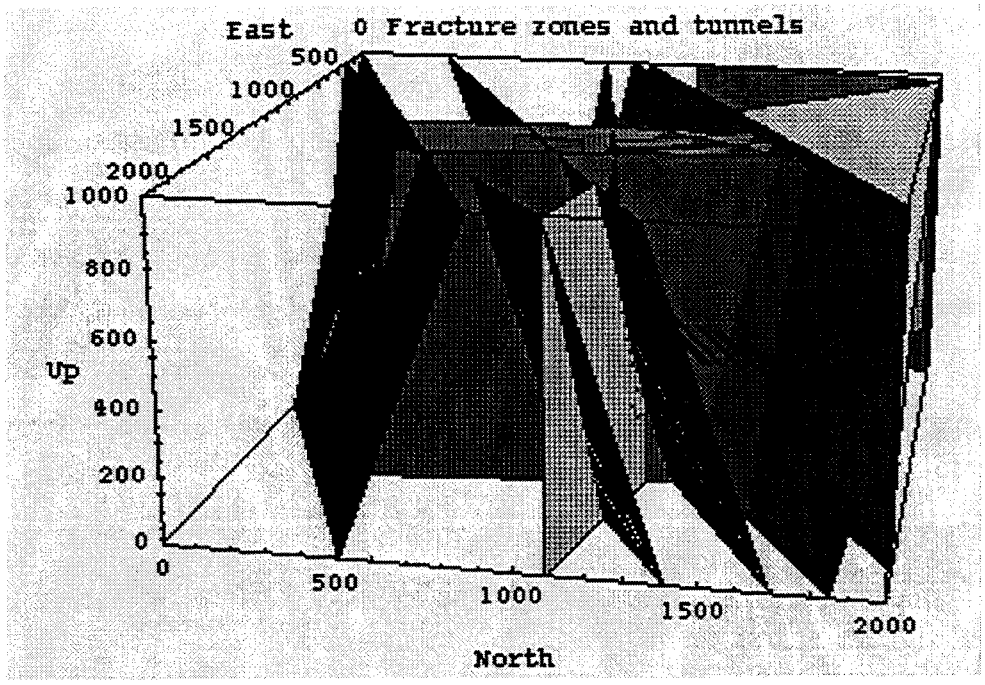

Figure 1. All the fracture zones within the model region. The locations of the tunnels in block 4 are also indicated.

3.4 Field data and scaling of rock mass conductivity

For the Aberg site, hydraulic measurements carried out using a distance between packers of 3 m are available from Sicada. In order to obtain the rock mass conductivity to be used in CHAN3D in the Alternative Model Project, the hydraulic conductivity measurements have to be scaled to the length-scale used in the modelling. Here, a channel length of 30 m was used.

In order to do this, the 3 m packer data from Äspö HRL were used. First, the data points that belong to the rock mass were selected. To exclude the data points that belong to the fracture zones, the distance between the measurement point and the planes defining the fracture zone are determined. If this distance is less than the half of the fracture zone thickness the data point is eliminated, as it is assumed to belong to the fracture zone.

From these data, the mean hydraulic conductivity is calculated. In this case, the geometric mean is calculated (i.e. mean of $\log_{10}(K)$). The value of the mean hydraulic conductivity for the mass rock is $2.0 \cdot 10^{-10}$ m/s. The standard deviation in $\log_{10}$-scale is 1.5.

In order to determine the scaling factor, mean values were calculated using a moving window with a length of 30 m. A hydraulic conductivity of about -8.5 in the $\log_{10}$ -scale and a standard deviation of about 0.8 were obtained. These values are influenced by the criteria used to decide whether a point belongs to the fracture zone or to the mass rock. When the points are assigned, some locations with large hydraulic conductivity may be included as rock mass and some points with very small hydraulic conductivity may be included as fracture zones.

Alternatively, hydraulic conductivity values can be taken directly from Rhén et al. (1997). For a scale of 30 m, the $\log_{10}$ value for the hydraulic conductivity is -8.2 and the standard deviation about 0.9. Differences between mass rock and fracture zones do not appear to be considered.

A third alternative was also explored. Here, a large number of data points were generated with $\log_{10}(K_g) = -10.0$ to simulate 3 m packer data. It is assumed that the conductivities follow a log-normal distribution, no spatial correlation was considered. The data was gathered in 30 m sections and the resulting mean and standard deviation were calculated. The procedure was performed for standard deviations between 0 and 1.6. The results from this scaling exercise are shown in Figure 2. The use of a moving window technique on the generated data set was also tested. No significant differences were obtained between the method using the moving window and the method not using the moving window.

From 3 m packer data for the rock mass (fracture zone data excluded), the mean value of $\log_{10}(K_g) = -9.70$ with a standard deviation of 1.5 on the $\log_{10}$-scale. From the numerical up-scaling study, a scaling factor of 1.5 was calculated, giving a mean hydraulic conductivity for 30 m packer test about 30 times larger than the mean hydraulic conductivity for 3 m packer test. The $\log_{10}$ value of the mean hydraulic conductivity is then -8.2. Improved agreement could be achieved if spatial correlations were included in the generation of the 3 m conductivities.

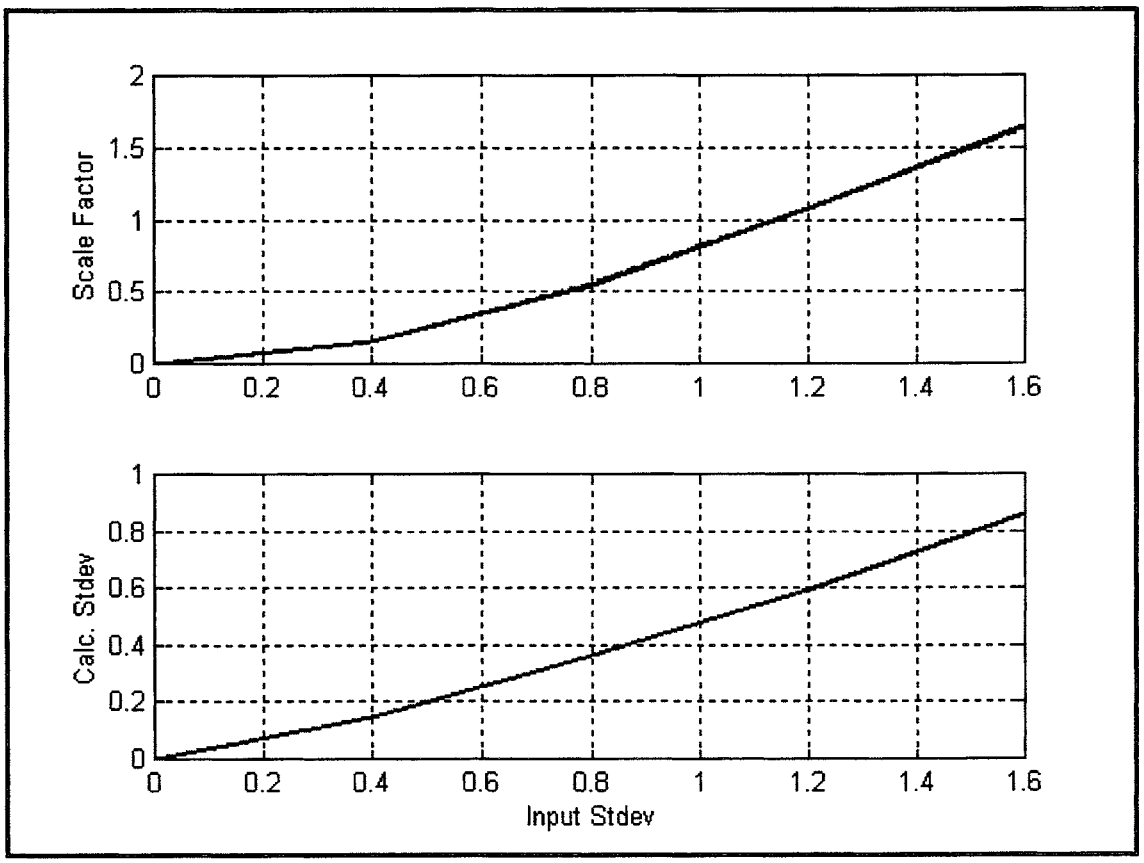

Figure 2. Increase in scale factor and calculated standard deviation with increasing input standard deviation. The number of randomly generated data points was 100 000.

3.5 Study of fracture-zone transmissivity

When a 2-D structure with variable hydraulic conductivity is generated, the resulting hydraulic conductivity (effective hydraulic conductivity) is equal to the geometric mean of the hydraulic conductivity in the structure (Marsily, 1989). For a 3-D structure the effective hydraulic conductivity is larger than the geometric mean. For a fracture zone, where only a few elements are used to describe the thickness, it is not clear if the relationship for a 3-D model is applicable.

To illustrate the effect of the standard deviation on the effective hydraulic conductivity for a fracture zone a set of simulations were performed. In the test, the flow rate was calculated in a

single fracture zone for different values of standard deviation in $\log_{10}$-scale using CHAN3D. As a base for the mean value a transmissivity of $T = 1.0^{-6}$ m^2/s was used. The width of the fracture zone was 60 m. Figure 3 shows the ratio between the actual flow rate in the fracture zone for increasing standard deviation and the value for a homogeneous porous medium (St dev = 0). The ratios between the effective hydraulic conductivity obtained in the simulations and the geometric mean were calculated. In Table 5, these values were compared with the ratio between the theoretical effective hydraulic conductivity for a three-dimensional porous medium and the geometric mean. From these values, it is concluded that the fracture zone behaves almost as a 3-D structure. CHAN3D uses a factor to compensate for the increase in conductivity.

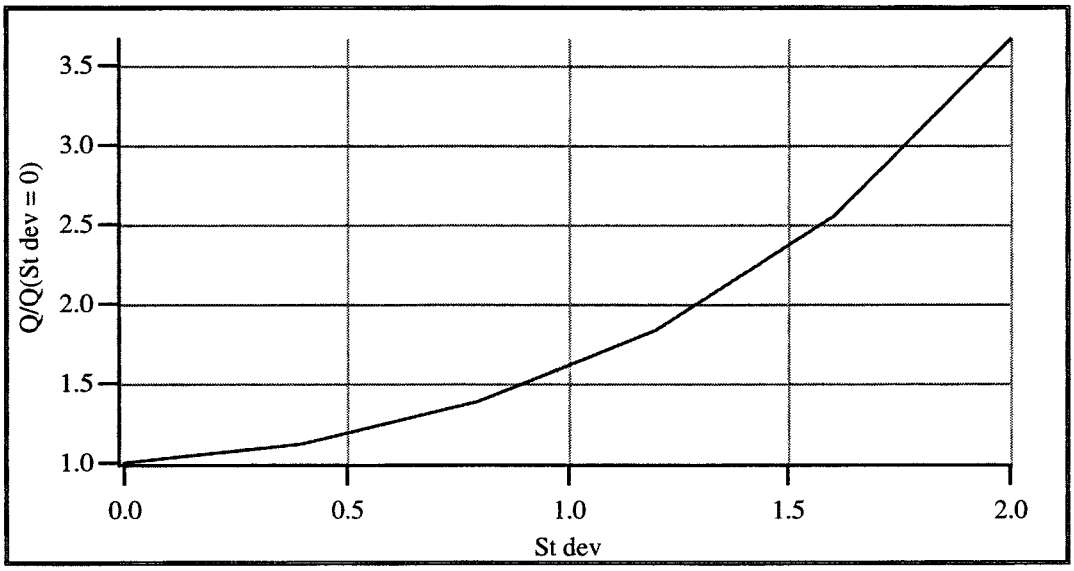

Figure 3. Increase in flow rate with increasing standard deviation. The flow rates are compared with the flow rate in the fracture zone obtained when the standard deviation in conductance is zero.

Table 5. Simulated values of the flow rate and effective conductivity for different standard deviations, in comparison with the theoretically calculated flow rate and the geometric mean, K_g.

St Dev	$Q_{Sim.}/Q_{Theor.}$	$K_{Sim.}/K_g$
0.0	1	1
0.4	1.12	1.14
0.8	1.38	1.56
1.2	1.84	2.27
1.6	2.55	3.26
2.0	3.67	4.53

3.6 Flow-wetted surface

In order to determine the flow-wetted surface area, the intersection frequency between boreholes and fractures in the rock is used. Using borehole data from the Äspö site, the total number of packers with conducting features within the fracture zones is found to be 727 and the total intersection length between the boreholes and the fracture zones is 2 418 m. From these borehole data, an intersection between a borehole and a fracture with an open channel is found about every 3.3 m. Thus, the borehole diameter, D_{bh}, and the average distance between the channels, H, are the only known entities.

To obtain the flow-wetted surface area, let us consider a rock volume with a number of channels randomly distributed in the space. It is assumed that the channels have a length L, a width W, and an area A. A borehole drilled through this rock mass will intersect, on the average, a channel each H m. To correlate the number of channels in a given rock volume to the frequency that channels are intersected by a borehole the average channel areas are projected on a plane perpendicular to the borehole. The projected areas are redistributed over this plane with a separation between them equal to the borehole diameter. Thus the average projected area, A_o, needed for a channel to be intersected by a borehole is:

$$A_o = A_{proj} + (W_{proj} + L_{proj})D_{bh} + D_{bh}^2 \qquad (2)$$

This area includes the projection of the channel area and the space occupied by the borehole itself. Since the channels can be randomly oriented in space, the mean value of the projected lengths and widths of the channels in a plane are $L_{proj} = (\pi/4)L$ and $W_{proj} = (\pi/4)W$. The value of the projected area of a channel is A/2. (In a previous paper (Moreno et al. 1997) we have used an approximate solution to estimate the projected area, instead of the solution presented here). If the average distance between channels intersected by the borehole has been obtained as H, then the average rock volume containing one channel is $H \cdot A_o$. The specific flow-wetted surface area, a_R, is the surface of the channel, 2A, in the rock volume $H \cdot A_o$. Thus, if when the term D_{bh}^2 is neglected:

$$a_R = \frac{2 \cdot A}{H\left[\frac{A}{2} + \frac{\pi}{4} D_{bh}(W+L)\right]} \qquad (3)$$

If the length and width of the channels is large compared with the borehole diameter, the flow-wetted surface area may then be determined as a function of only the distance H, $a_R = 4/H$. Otherwise, L or W must be determined. W is not known unless independent observations have been made, e.g. in drifts and tunnels. Fortunately the specific flow-wetted surface is not very sensitive to W and L. In this particular case, the value of H was estimated to be 3.3 m from the borehole information.

Therefore, the channel frequency, conductivity distribution and flow-wetted surface are obtained from interpretations of hydraulic packer tests. Summarising these entities, the specific flow-wetted surface area is 1.2 m^2/m^3. In our calculations we have used the estimated flow-wetted surface for the fracture zones and 10% of that value for fracture in the rock mass, since the estimation is based on fracture zone values.

3.7 Summary of the data evaluation process

The data evaluation process is summarized in Table 6. A more general data evaluation process is illustrated in the Appendix using the simulations of the LPT2 experiment as an example. Hydraulic conductivity data from Sicada, reinterpreted on a 3 m scale, were used to obtain raw data for the rock mass conductance and the standard deviation in conductance (for both rock mass and fracture zones). From the same data set, the fracture frequency was used to estimate the flow-wetted surface. The flow porosity was assumed, based on values used in other simulations using Aberg as the host rock.

Channels falling within the EDZ-domain are given a higher conductance. The available tunnel geometries are used to define the domain. We have assumed that the conductance of the EDZ is ten times higher than the mean for the rock mass. If a fracture zone intersects a channel in the EDZ, it is conservatively assumed that the fracture zone determines the local conductance. There is information available on the influence of excavation on the rock conductivity. However, the excavation technique was not studied in the project and was therefore not defined. Also, more work may have to be done on how to interpret the available data to improve the modelling of the EDZ.

The flow-wetted surface area is estimated from the 3 m packer data taken from Sicada. The information we have used to calculate a_R is from fracture zones and therefore we have used 10% of that value for the rock mass domain to account for the presence of less conducting fractures. For the EDZ, 30% of the a_R-value is used. The factor for the EDZ has little influence since a limited amount of channels are traversed in this domain.

Table 6. Summary of the data evaluation process.

Model Entity	**Source**	**Type of Data**
Rock mass conductance	Sicada	3 m packer data
Fracture zone conductance	Delivery 2 *	Transmissivity data
Standard deviation in conductance	Sicada	3 m packer data
Geometry of fracture zones	Delivery 2	Plane equation
Geometry of tunnels	Delivery 1 *	Coordinates
Canister positions	Delivery 1	Coordinates
Boundary conditions	Delivery 2	Fresh water head
Flow-wetted surface	Sicada	3 m packer data
Flow porosity	Assumed	
Factor for EDZ	Assumed	

* Data delivery 1 contained information on model region, fracture zone geometry, tunnel and canister positions, and also a definition of the project (Ström, 1997a). Data delivery 2 contained an update of the fracture zone information (Ström, 1997b).

4 ENTITY CALCULATIONS USING CHAN3D

One of the concepts behind the Channel Network model and the corresponding code CHAN3D is that flow and transport take place in channels in the rock. This is based on field observations from boreholes and tunnels. Most of the flow and transport takes place in fracture zones. The fracture zones are represented by channels with a log-normally distributed conductivity, the mean value corresponding to the measured transmissivity. The standard deviation of the conductivity is estimated from the measured hydraulic conductivity data. The rock mass is represented by channels taken from a distribution with a lower mean conductivity value. The standard deviation used is the same as that for the fracture zones. In addition, the obtained fracture-zone data may be used to obtain a frequency for conducting channels or a mean distance, H, between conducting fractures.

CHAN3D uses a specific flow-wetted surface, a_R, estimated from borehole data. Since this a_R is estimated from fracture zone data, channels within the fracture zones are given a flow-wetted surface, FWS, based on a_R, whereas channels in the rock mass are given a smaller flow-wetted surface. A value of 10% of the value for fracture-zone channels is used for the FWS for the channels in the rock mass, based partly on field data (Gylling et al. 1998a). This value is somewhat arbitrary. It is possible to assign an individual FWS to each channel, but since the experimental data is not sufficient to obtain statistics for the spatial distribution of a_R, one value of FWS is used for channels in the fracture zones and one value of FWS is used for the channels in the rock mass.

If we have assigned an FWS to each channel and calculated the flow distribution in the channel network we can obtain an F-value for each channel. For each flow path from the repository to the release point, the individual F_i values may be added to obtain F_{tot}.

4.1 Estimates of $\bar{a}_w$ and t_{tot} for a transport path

Our approach to calculating the "equivalent" FARF31 parameters from the CHAN3D calculations is to:

- use Equation 4.1 (in Andersson et al. 1998) to calculate a_R based on conductive fracture frequency data
- derive the transport paths from each canister of interest in the repository to the release points
- for each transport path, i, calculate;

  - $t_{tot,i} = \{\sum t_j\}_i$
  - $F_{tot,i} = \{\sum (FWS)_j / q_j)\}_i$
  - $\bar{a}_{w,i} = F_{tot,i}/t_{tot,i}$

where j ranges from 1 to the number of channels traversed along each path. Equivalent parameters to FARF31 for a specific canister location are then t_{tot} and $\bar{a}_w$.

4.2 The Peclet number

Due to the Channel Network concept, dispersion is a simulation result caused by the heterogeneous flow distribution and interaction mechanisms in the model. This means Pe is not needed as an input parameter to CHAN3D. For non-interacting solutes the Pe may be estimated from the residence time distribution for particles from a given canister. Since the Pe calculated for non-interacting solutes is not applicable for interacting solutes, for predictions with interacting solutes a Pe will be assumed.

The following steps are proposed in this study to address the dispersion for sorbing solutes (Andersson et al. 1998):

1. Regard dispersion as an uncertain macro-parameter and study its importance
2. In a base case, assume the dispersion length always to be 10% of the travel path i.e. Pe=10
3. Study to what extent the results are robust with regard to Pe-numbers (Base case Pe=10, other cases 2 and 50).

In this study CHAN3D was used a bit different than in previous studies. One new task was to produce input data to FARF31, which is restricted to one stream tube from each canister position. Producing input data to COMP23 has been performed before in the CHAN3D-COMP23 coupling studies (e.g. Gylling et al. 1998a) where the transport part of CHAN3D was used to simulate the far field transport. In the normal use of CHAN3D a large number of particles from each starting position are released to simulate a plume of solutes subjected to advection, hydrodynamic dispersion and interaction mechanisms. In this study, only 200 particles were used to model a single stream tube from each release position. This implies that the travel time for water for a stream tube is the median of the 200 particles exiting at the ground surface. For the calculations of the release locations at the ground surface, the centre of gravity of those initially 200 particles was used.

5 RESULTS

In each realisation all the individual entities for the flow paths originating from the canister positions are recorded. To represent the repository 229 canister positions are studied. The individual values are then post-processed into ensemble statistics. In the end of each realisation statistics for the specific realisation are calculated for the post-processing of the performance measures. At present 30 realisations have been made. In all realisations, entities in the form $y = \log_{10}(x)$ are calculated, where x represents:

- Darcy velocity, q, [m/year]
- Travel time, t, [year]
- F-ratio, F, [year,m^2/m^3]
- Flow-wetted surface, a_w, [m^2/m^3 water]

In order to summarise the ensemble of realisations, the mean, the variance, the median and the percentiles for 5 and 95 % are calculated. In addition, a measure of the spreading of the results is also calculated; the "dispersion". Dispersion is defined as $D_y=y_{95\%}-y_{5\%}$.

The results are presented as ensemble statistics over all values obtained in the 30 realisations. The following section also presents release locations from a single realisation, statistics for two typical realisations, statistics for three interesting canister positions and as performance measures. The results are shown in tables and figures (histograms) below.

5.1 Ensemble statistics

The ensemble statistics are calculated using all the individual values obtained in the realisations, i.e. for each entity there are 30 times 229 values. The ensemble results for Darcy velocity at repository scale, water travel time, and F-ratio, for the flow paths are shown in Table 7. The table

shows the mean value, variance, median, 5th and 95th percentiles and spread of all the entity values obtained in the 30 realisations. Histograms of these ensemble values are shown in Figures 4 - 7.

Table 7. Summary statistics for the ensemble of the entities.

	Darcy velocity Fractures	T-water	F-ratio	a_w
Mean	-3.133	1.025	4.831	3.800
Variance	0.468	0.193	0.216	0.039
Median	-3.260	1.033	4.869	3.757
5th Percentile	-4.017	0.238	3.948	3.563
95th Percentile	-1.654	1.667	5.404	4.153
Spread, D_y	2.363	1.429	1.456	0.590

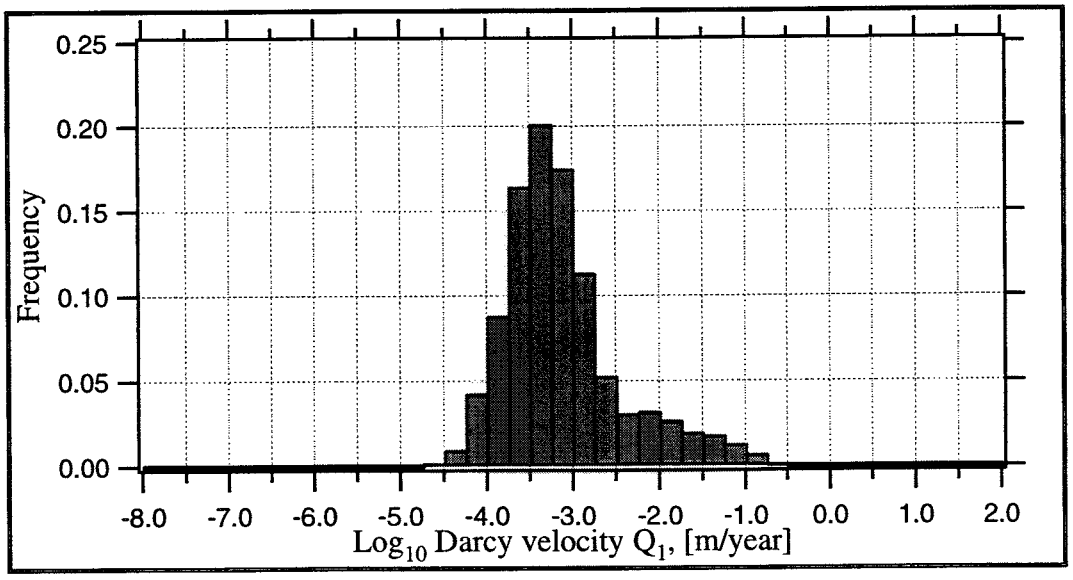

Figure 4. Relative frequency histogram of $\log_{10}$ Darcy velocity around the canister deposition hole. Results for the ensemble of all realisations.

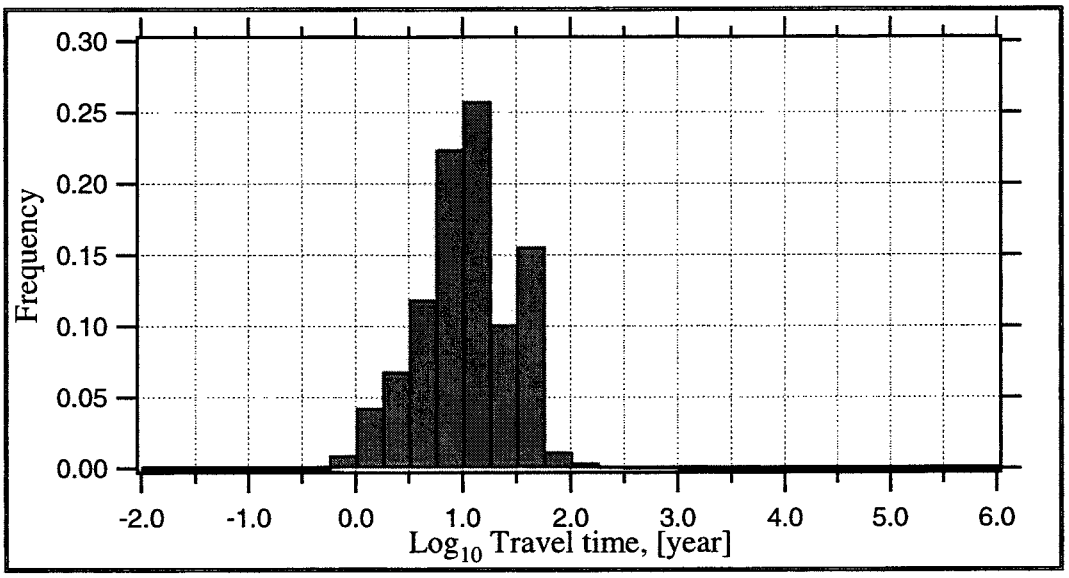

Figure 5. Relative frequency histogram of $\log_{10}$ travel time for water from the repository to the interface between geosphere and biosphere. Results for the ensemble of all realisations.

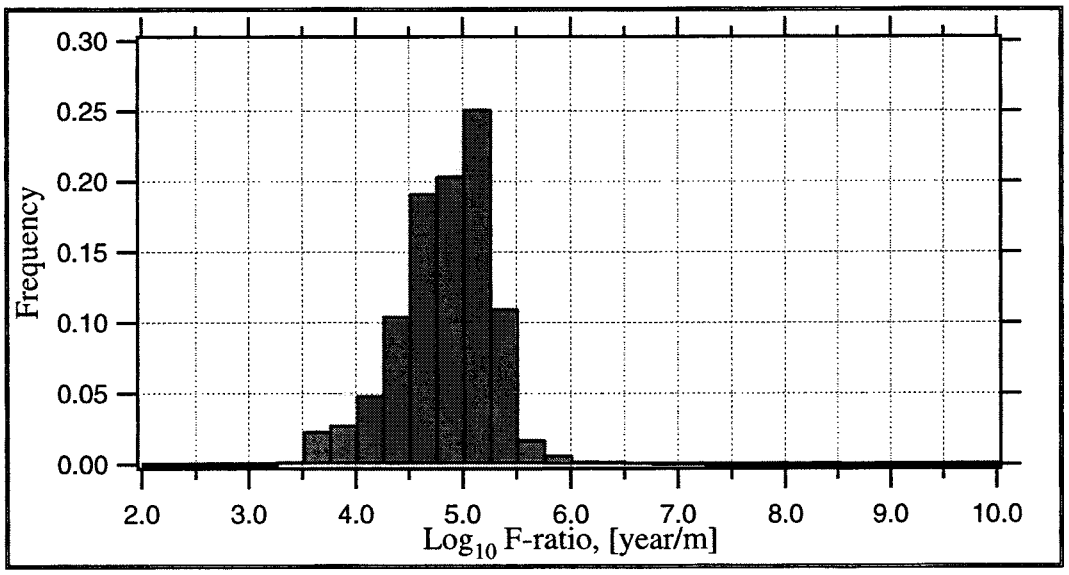

Figure 6. Relative frequency histogram of $\log_{10}$ F-ratio for flow paths from the repository to the interface between geosphere and biosphere. Results for the ensemble of all realisations.

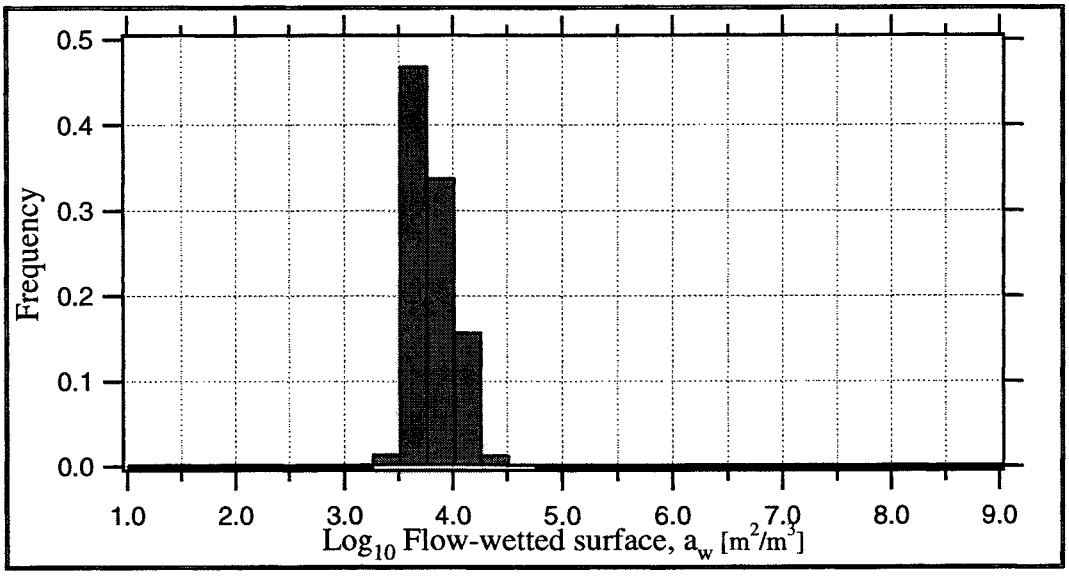

Figure 7. Relative frequency histogram of $\log_{10}$ flow-wetted surface for flow paths from the repository to the interface between geosphere and biosphere. Results for the ensemble of all realisations.

5.1.1 Flux in the excavated disturbed zone and flow-wetted surface, a_R

In addition to the requested entities we have calculated the Darcy velocities in the excavated disturbed zone around the deposition tunnels and the flow-wetted surface area based on the volume of rock, a_R. The results are shown in Table 8. We have modelled the EDZ with a ten times higher conductivity than the rock mass. A histogram over the ensemble of flux values in the EDZ is shown in Figure 8.

Using the specific flow-wetted surface, estimated from borehole data with the method outlined in Section 3.6, as input data, it is possible to calculate statistics of the magnitude of the flow-wetted surface in the traversed paths. Since fracture zone data where used in the preparation of input data, channels that belong to fracture zone domains in the model are assigned properties related to

the specific value. For the rock mass domain, we have assumed that the value of flow-wetted surface area is ten times lower. The distribution of a_R values may indicate to what extent the flow paths are located in fracture zones or in the rock mass. A histogram over the encountered flow-wetted surface values in the flow paths is shown in Figure 9. It can be seen that most path lines seem, at least to some extent, have been located in fracture zones, whereas for about 15% of the path lines the rock mass dominates.

Table 8. Summary of the results for the Darcy velocity in the excavated disturbed zone and the flow-wetted surface based on volume of rock (a_R is not in log-scale).

	Darcy velocity EDZ	a_R [m^2/m^3 rock]
Mean	-3.251	0.669
Variance	0.324	0.066
Median	-3.224	0.729
5^{th} Percentile	-4.196	0.128
95^{th} Percentile	-2.324	0.979
Spread, D_y	1.872	0.851

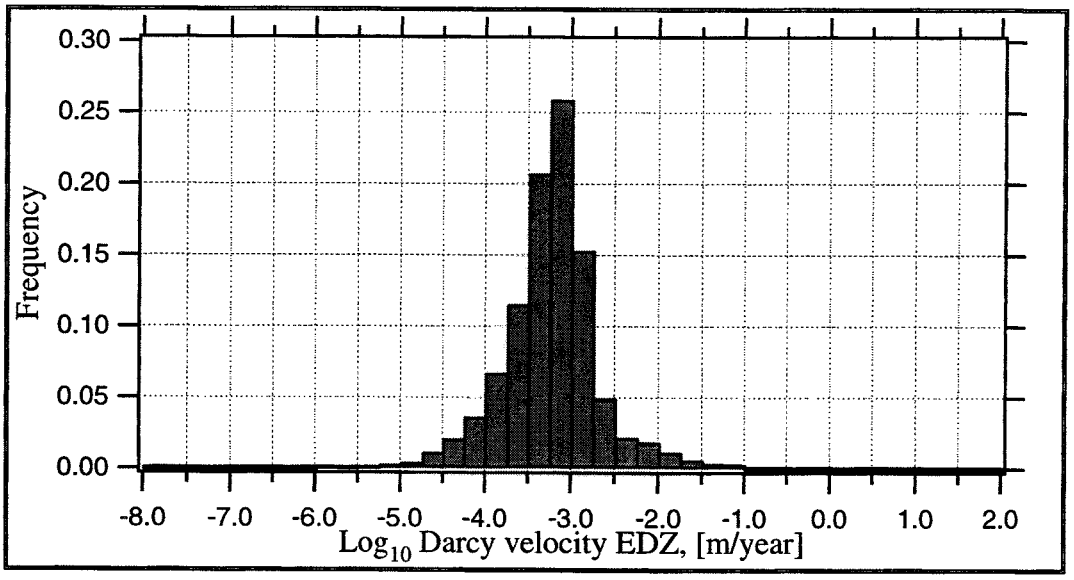

Figure 8. Relative frequency histogram of $\log_{10}$ Darcy velocity in the excavated disturbed zone. Results for the ensemble of all realisations.

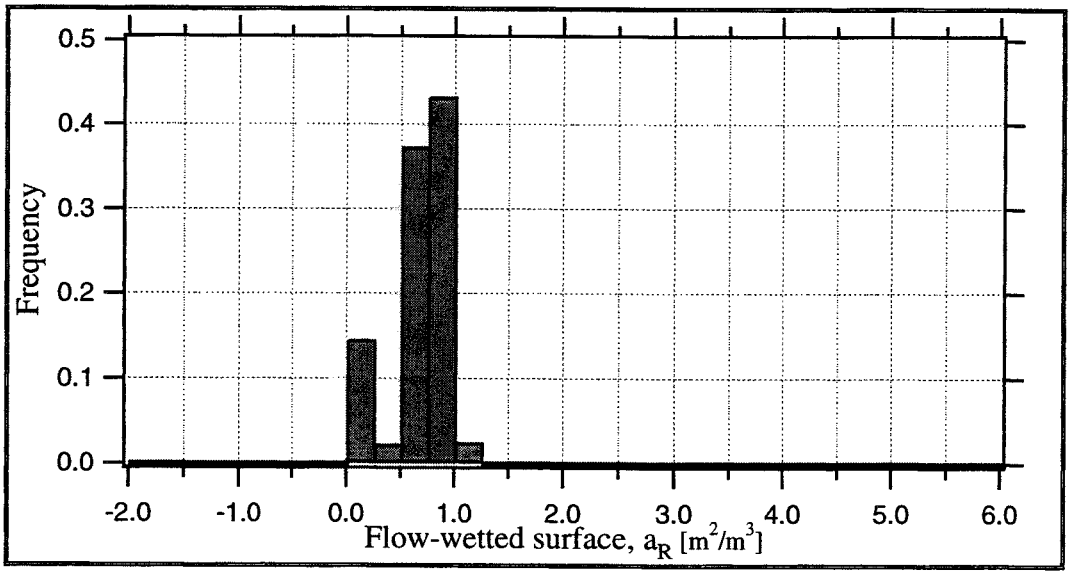

Figure 9. Relative frequency histogram of flow-wetted surface, a_R, for flow paths from the repository to the interface between geosphere and biosphere. Results for the ensemble of all realisations.

5.2 Release locations

In this study CHAN3D was used a bit different than in previous studies. In this study, only 200 particles were used to model a single stream tube from each release position. The centre of gravity of those initially released 200 particles were used for each simulated stream tube to calculate the release locations at the ground surface. The calculated exit locations of the stream tubes in one realisation are shown in Figure 10.

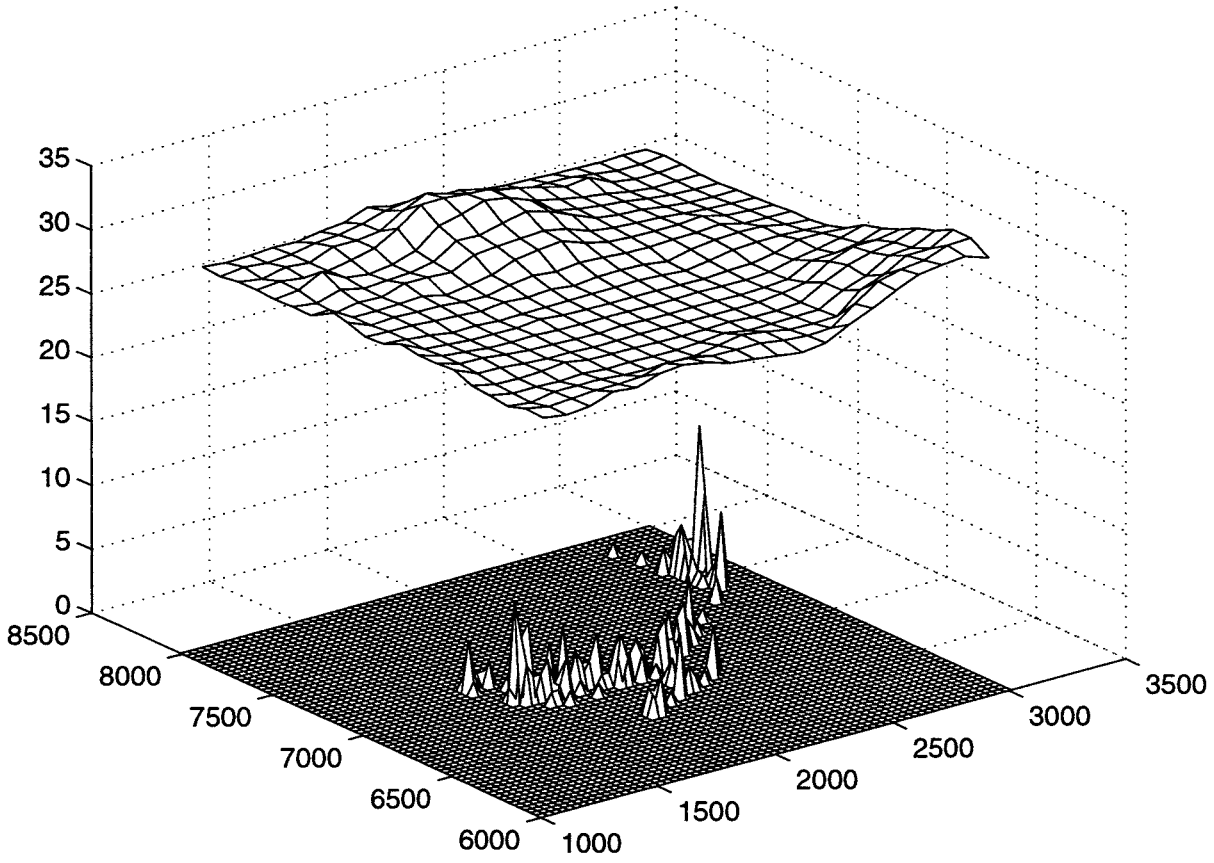

Figure 10. Release locations for the flow paths. The heights of the peaks represent the number of flow paths arriving at the locations. The boundary conditions on the top of the simulation domain are shown as an elevation plot (elevated about 25 units).

5.3 Typical realisations

Two criteria were used to find typical realisations. One was based on the median of travel time for water (Figures 11-15) and the second was based on Darcy velocity at canister locations (Figures 16-20). The summary statistics are in addition presented in Table 9 at the end of this sub-section. For both criteria, a search was made for the three realisations closest to the median of all realisations. From these three, the realisation with variance closest to the median of variances from the whole ensemble of realisations was chosen.

Based on water travel time

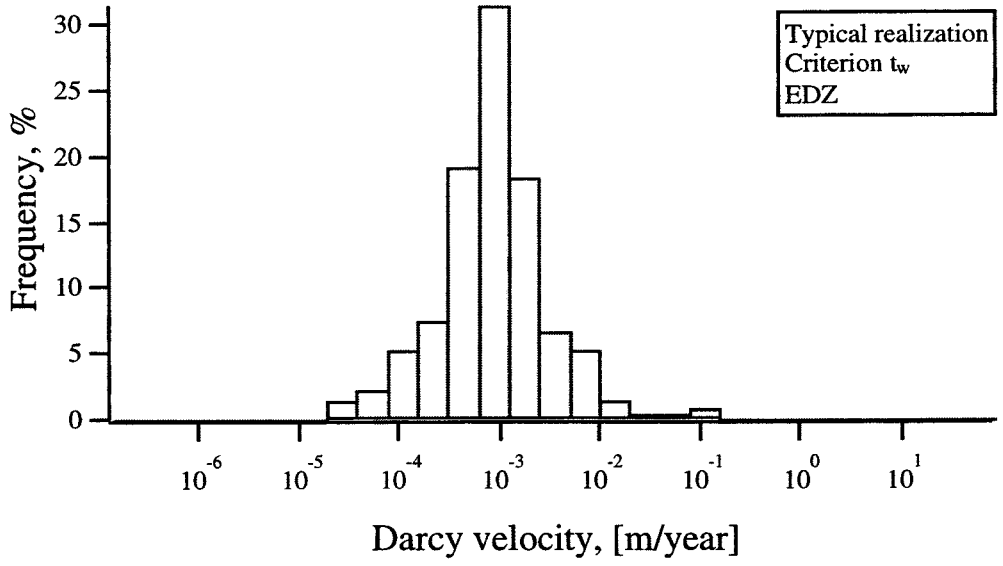

Figure 11. Histogram of Darcy velocities in the excavated disturbed zone, EDZ.

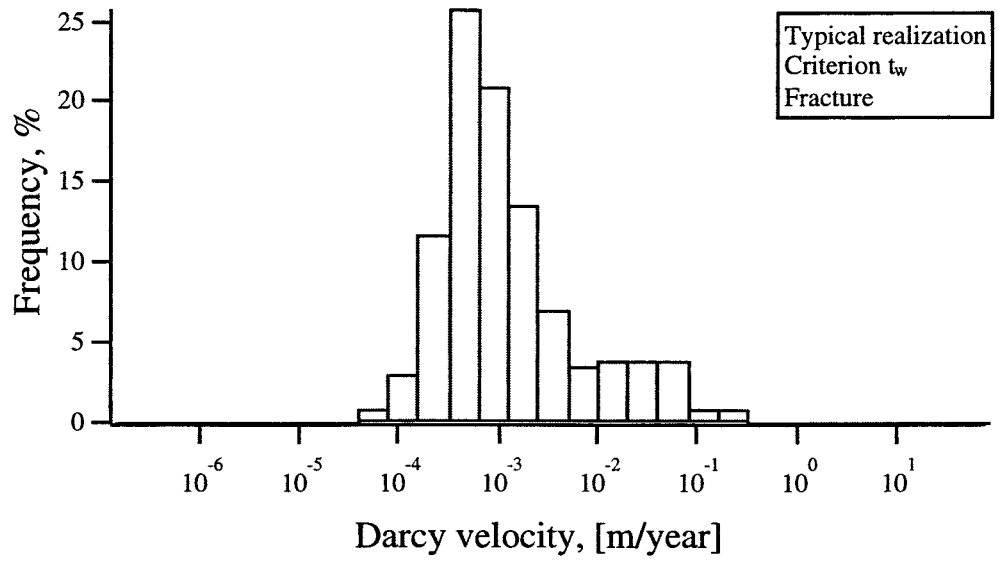

Figure 12. Histogram of Darcy velocities around the canister deposition hole.

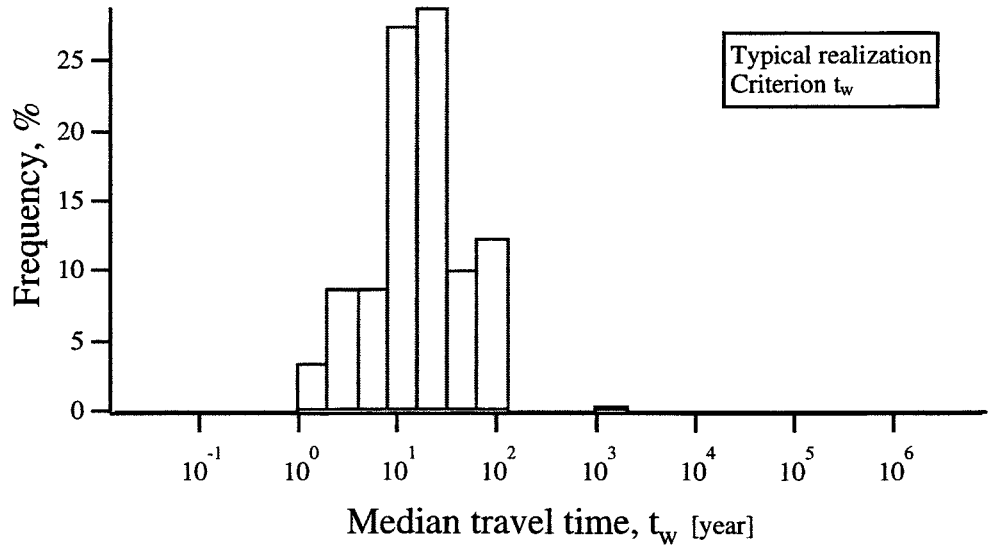

Figure 13. Histogram of travel time of water from the repository to the geosphere/biosphere interface.

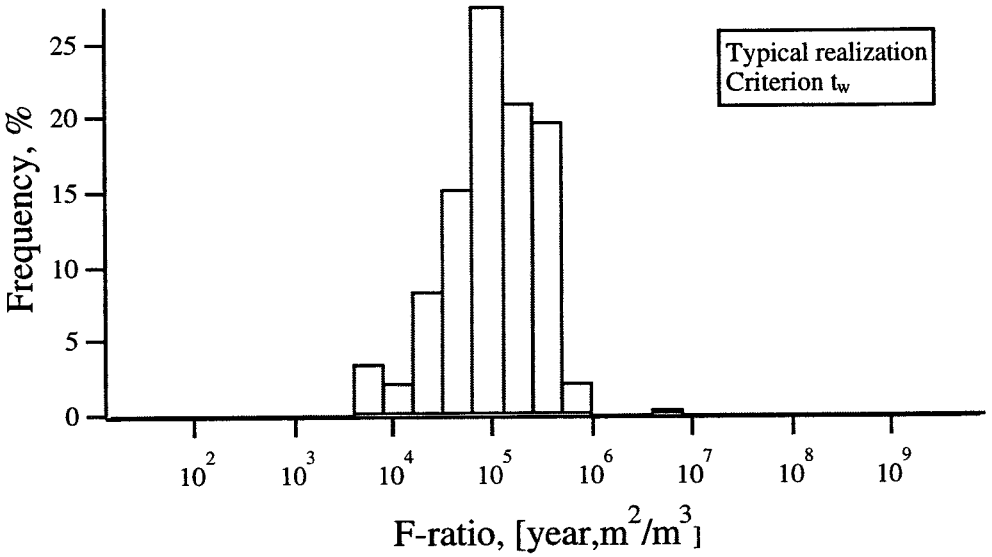

Figure 14. Histogram of F-ratio for paths from the repository to the geosphere/biosphere interface.

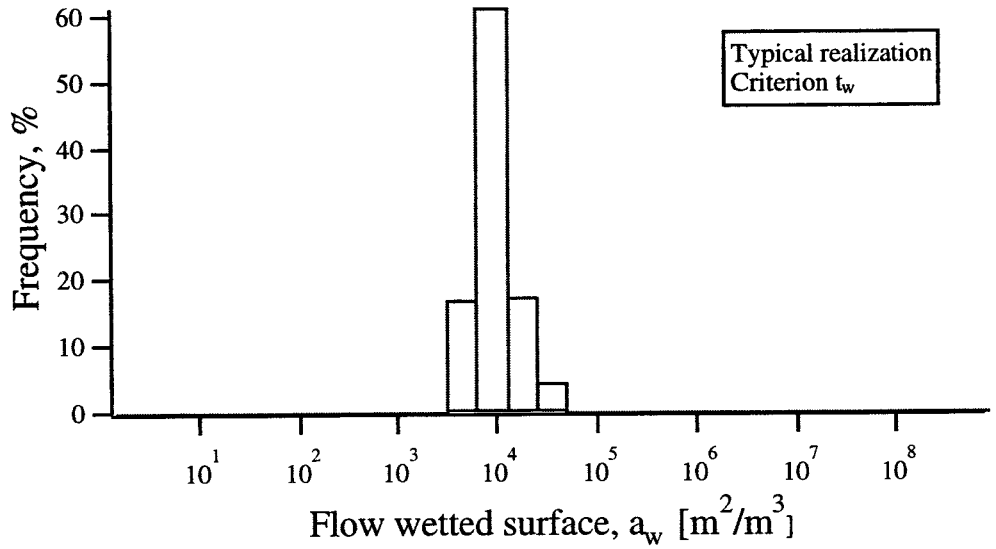

Figure 15. Histogram of flow-wetted surface based on volume of water for paths from the repository to the geosphere/biosphere interface.

Based on Darcy velocity

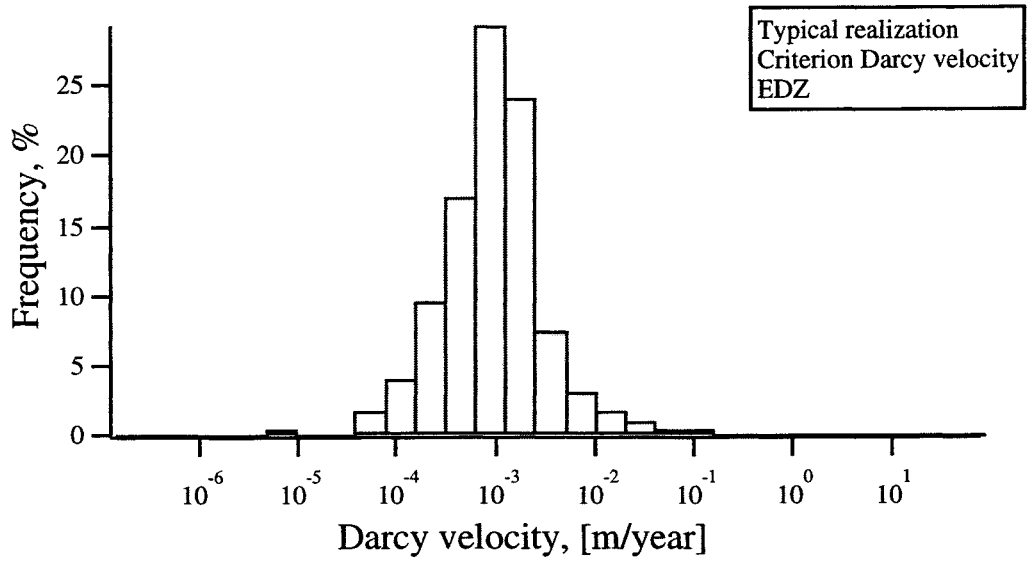

Figure 16. Histogram of Darcy velocities in the excavated disturbed zone, EDZ.

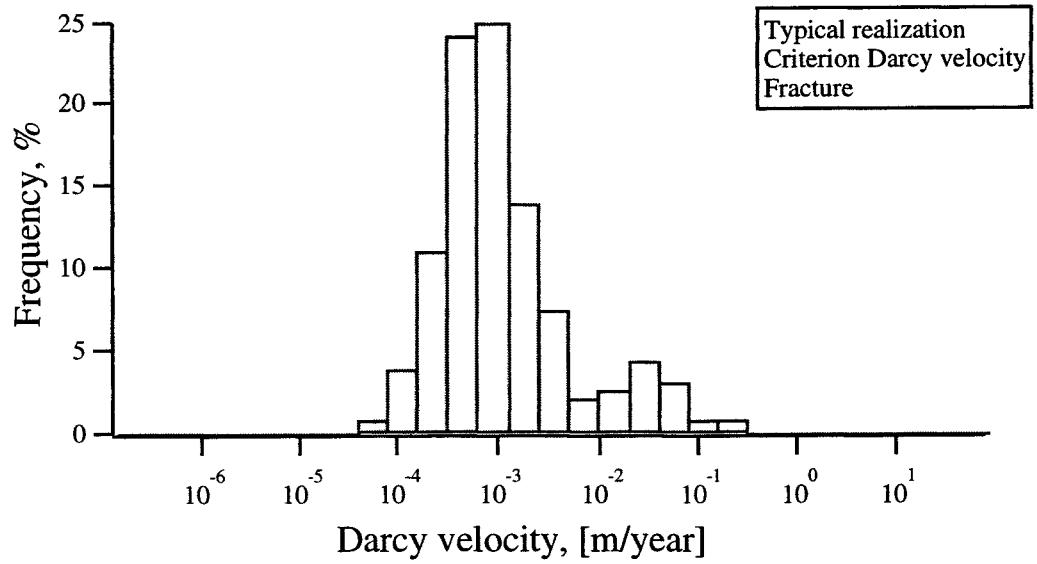

Figure 17. Histogram of Darcy velocities in the fractures at repository scale.

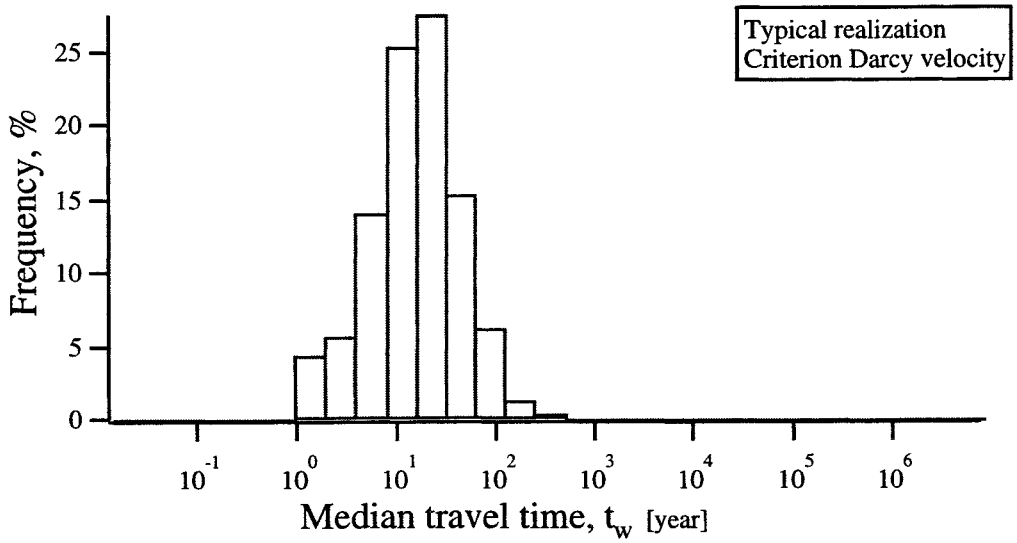

Figure 18. Histogram of travel time of water from the repository to the geosphere/biosphere interface.

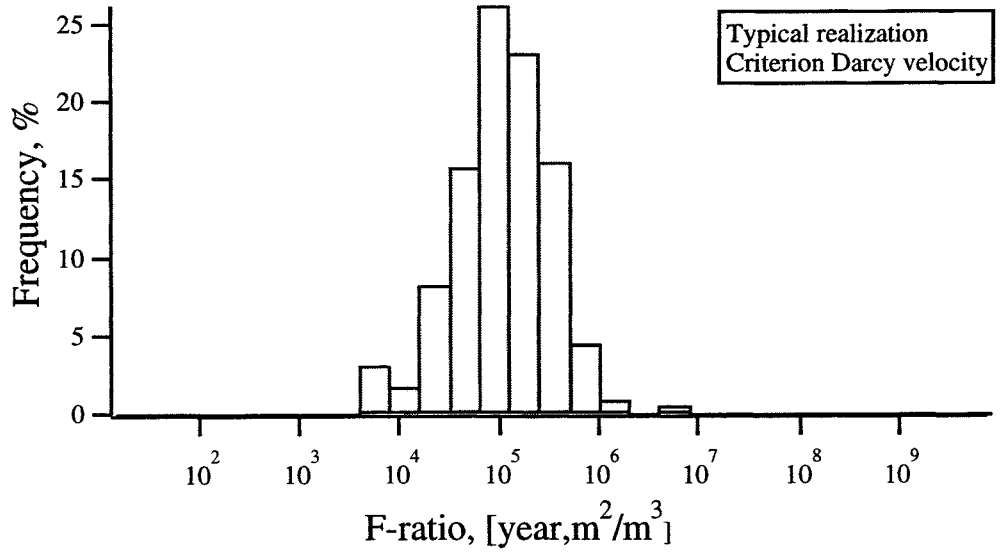

Figure 19. Histogram of F-ratio for paths from the repository to the geosphere/biosphere interface.

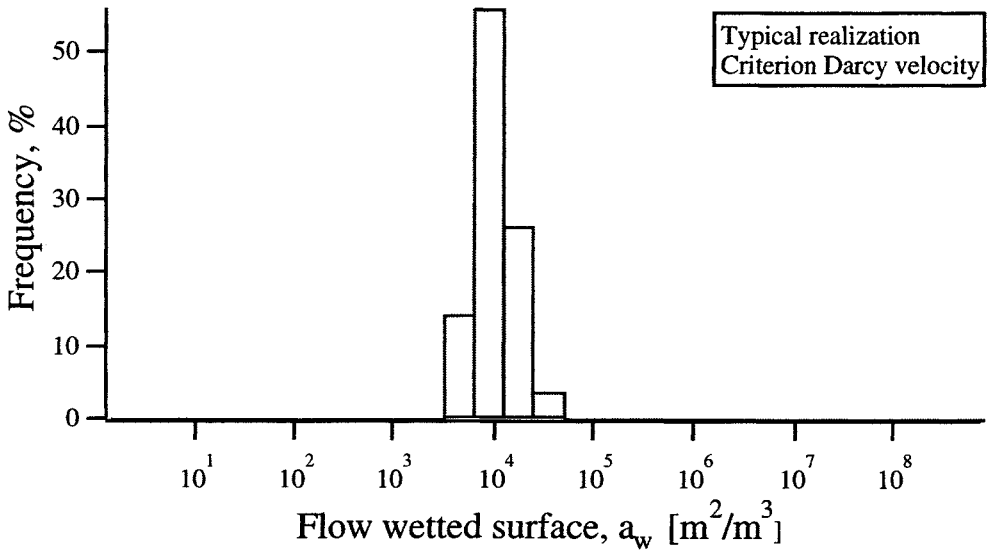

Figure 20. Histogram of flow-wetted surface based on volume of water for paths from the repository to the geosphere/biosphere interface.

Table 9. Summary statistics of travel times, F-ratio and canister flux for the two typical realisations.

	Based on t_w	**Based on q**
Travel time, t_w		
Mean t_w	1.019	1.002
Variance, t_w	0.208	0.201
Median, t_w	1.037	1.015
t_w, 5th percentile	0.172	0.114
t_w, 95th percentile	1.682	1.653
Dt_w	1.510	1.539
F-ratio, F		
Mean F	4.807	4.828
Variance, F	0.227	0.228
Median, F	4.846	4.867
F, 5th percentile	3.788	3.990
F, 95th percentile	5.442	5.525
D_F	1.654	1.535
Darcy velocity, q		
Mean q	-3.097	-3.128
Variance, q	0.505	0.462
Median, q	-3.261	-3.273
q, 5th percentile	-3.979	-3.991
q, 95th percentile	-1.492	-1.615
D_q	2.487	2.376

5.4 Interesting canister locations

Three canister positions of special interest were proposed, based on the HYDRASTAR calculations. The criteria for these positions were typical, short and long travel times. The coordinates for the canisters are given in Table 10. In general, the position for the short travel time was in good agreement with the CHAN3D simulations, whereas for the other two criteria there were often differences between the two concepts. Statistics for the entities of the three canisters are given in Tables 11 to 14.

Table 10. Proposed interesting canister positions.

Canister	Tunnel	Block	X	Y	Z	Time
168	5	3	1735.505	7192.642	-500	Typical
542	6	4	2311.888	7310.508	-500	Short
885	11	6	2084.132	6832.721	-500	Long

Table 11. Statistics of Darcy velocity around the deposition hole for the three studied canisters.

	Canister 168	Canister 542	Canister 885
Mean	-2.11	-1.14	-3.53
Variance	0.08	0.04	0.19
Median	-2.02	-1.13	-3.59
5^{th} Percentile	-2.56	-1.46	-4.26
95^{th} Percentile	-1.80	-0.91	-2.83
Spread, D_y	0.77	0.55	1.43

Table 12. Statistics of travel time around for the three studied canisters.

	Canister 168	Canister 542	Canister 885
Mean	0.75	0.02	0.98
Variance	0.12	0.01	0.18
Median	0.60	0.01	0.94
5^{th} Percentile	0.39	-0.06	0.52
95^{th} Percentile	1.24	0.13	1.27
Spread, D_y	0.84	0.19	0.75

Table 13. Statistics of F-ratio for the three studied canisters.

	Canister 168	Canister 542	Canister 885
Mean	4.64	3.73	4.74
Variance	0.14	0.06	0.32
Median	4.53	3.64	4.72
5^{th} Percentile	4.26	3.51	3.96
95^{th} Percentile	4.96	4.18	5.30
Spread, D_y	0.70	0.67	1.34

Table 14. Statistics of flow-wetted surface area, a_w, for the three studied canisters.

	Canister 168	Canister 542	Canister 885
Mean	3.87	3.69	3.73
Variance	0.04	0.03	0.04
Median	3.85	3.62	3.68
5th Percentile	3.66	3.57	3.44
95th Percentile	4.12	4.06	4.02
Spread, D_y	0.46	0.49	0.58

Histograms of the entities for the three studied canisters are shown below in Figures 21 to 24 for canister 168, Figures 25 to 28 for canister 542 and Figures 29 to 32 for canister 885.

Canister 168

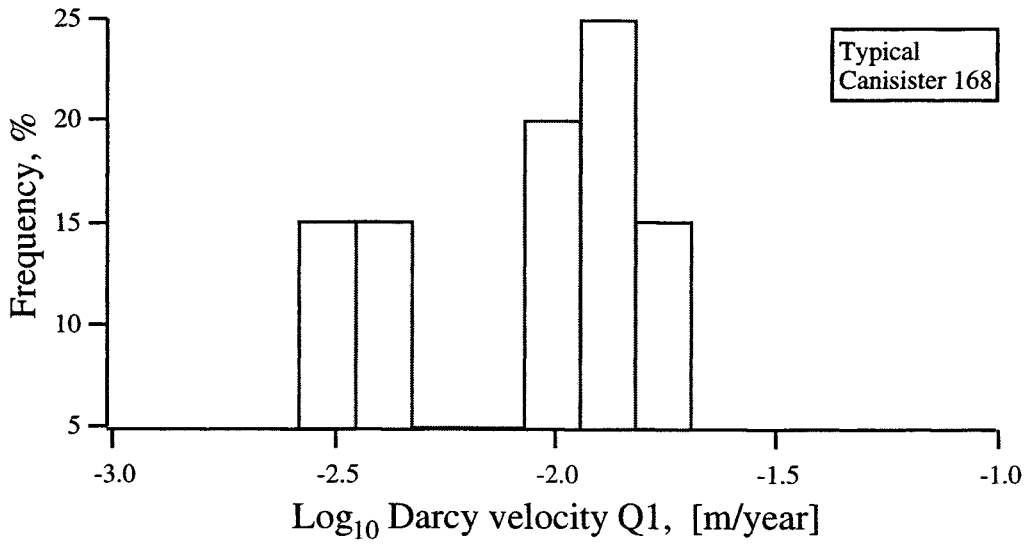

Figure 21. Histogram of Darcy velocities in the fractures at repository scale for canister 168.

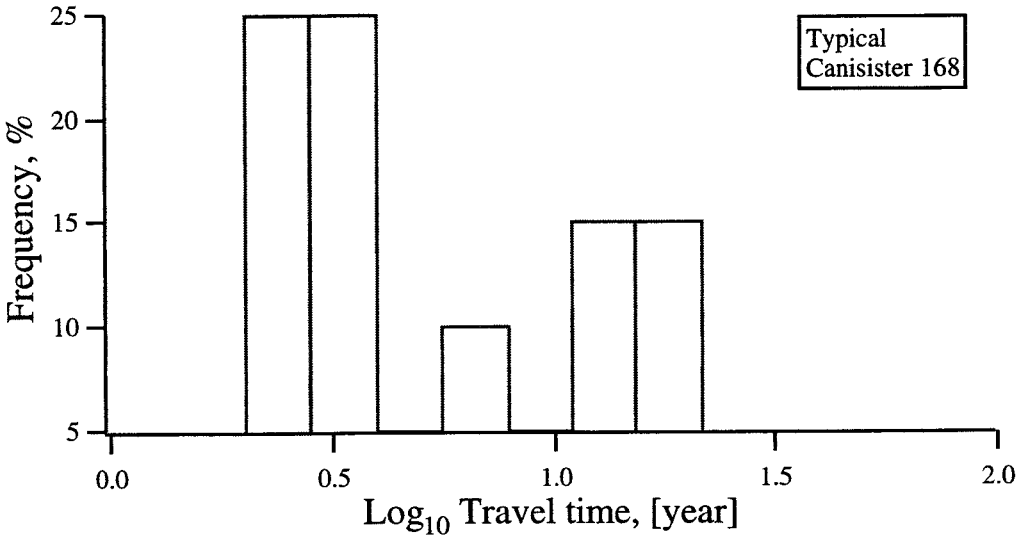

Figure 22. Histogram of travel time of water for canister 168.

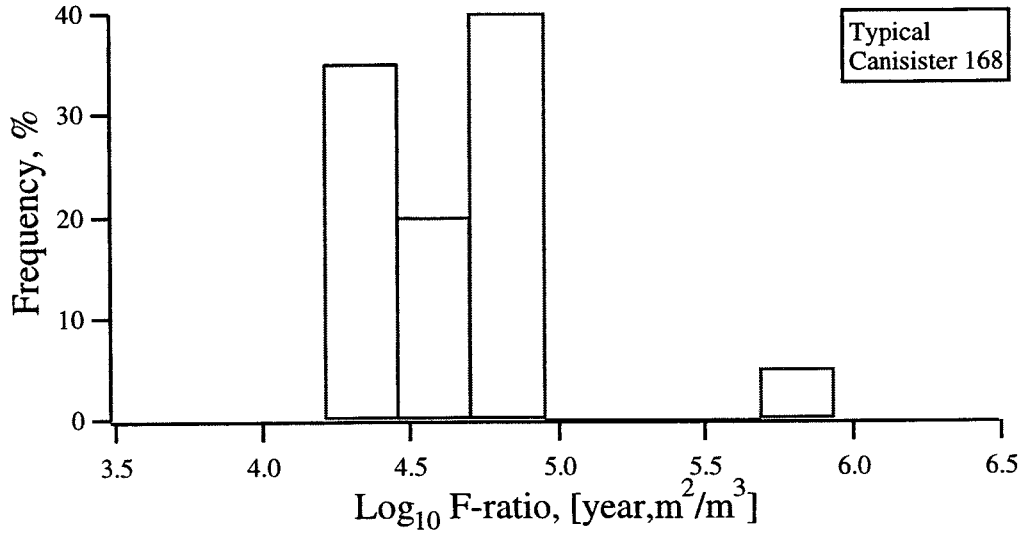

Figure 23. Histogram of F-ratio for canister 168.

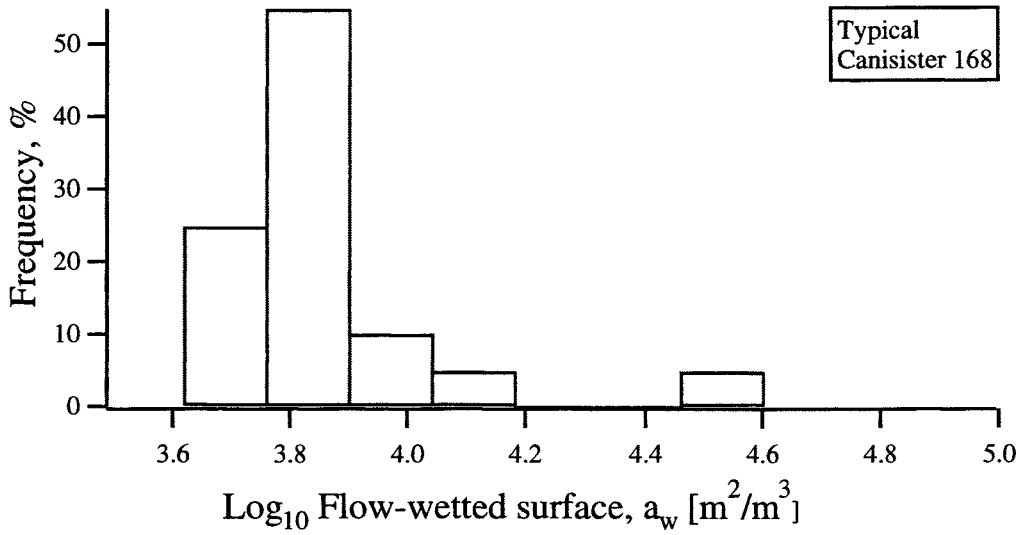

Figure 24. Histogram of flow-wetted surface based on volume of water for canister 168.

Canister 542

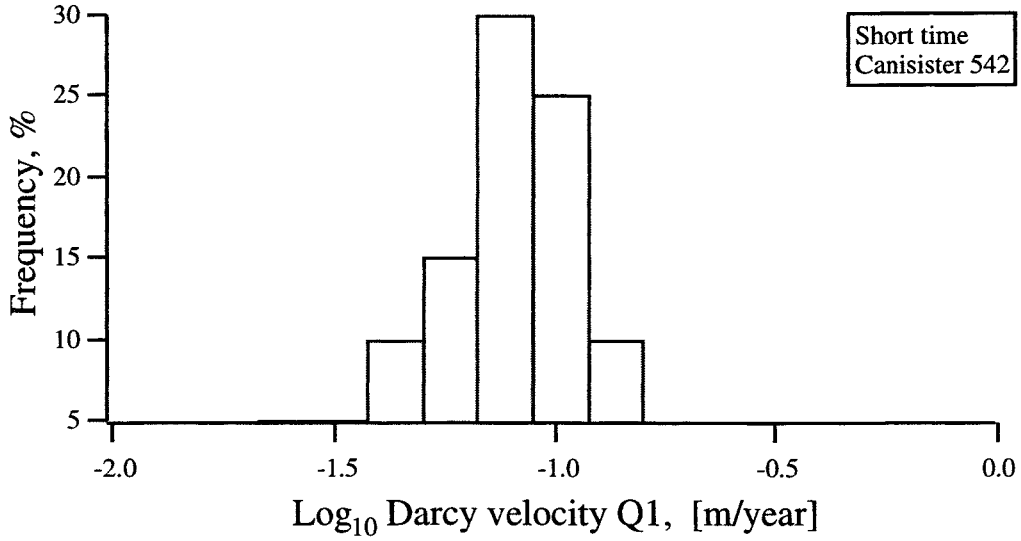

Figure 25. Histogram of Darcy velocities in the fractures at repository scale for canister 542.

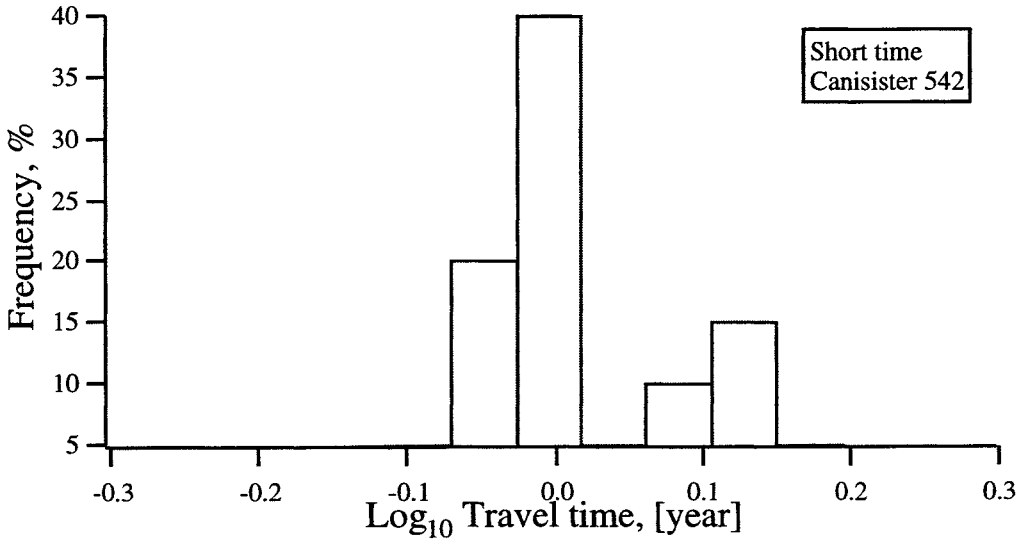

Figure 26. Histogram of travel time of water for canister 542.

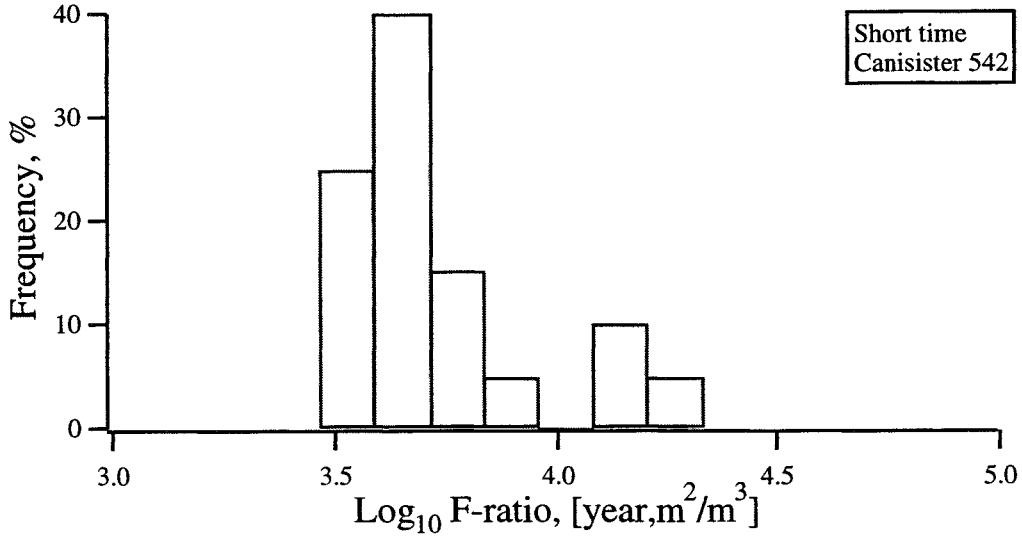

Figure 27. Histogram of F-ratio for canister 542.

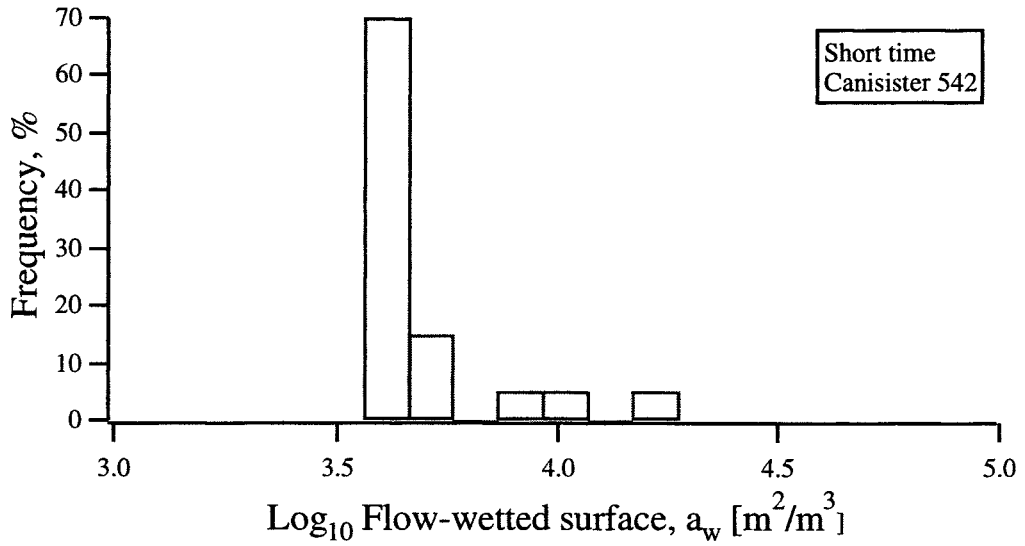

Figure 28. Histogram of flow-wetted surface based on volume of water for canister 542.

Canister 885

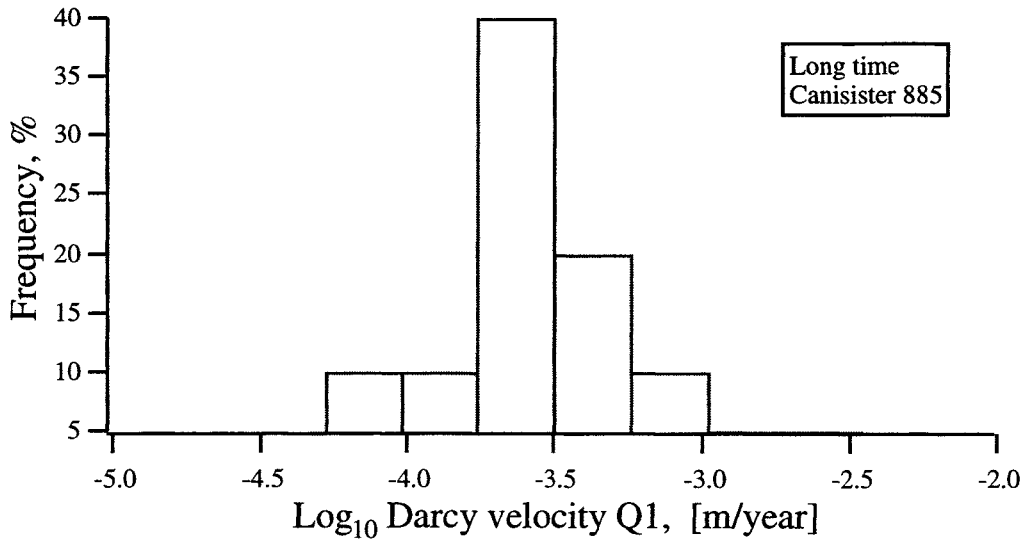

Figure 29. Histogram of Darcy velocities in the fractures at repository scale for canister 885.

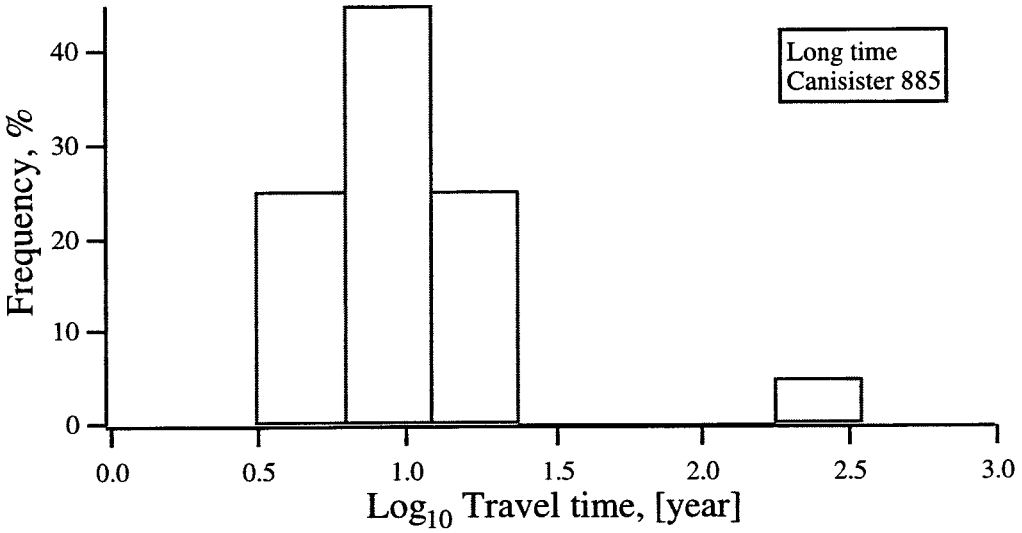

Figure 30. Histogram of travel time of water for canister 885.

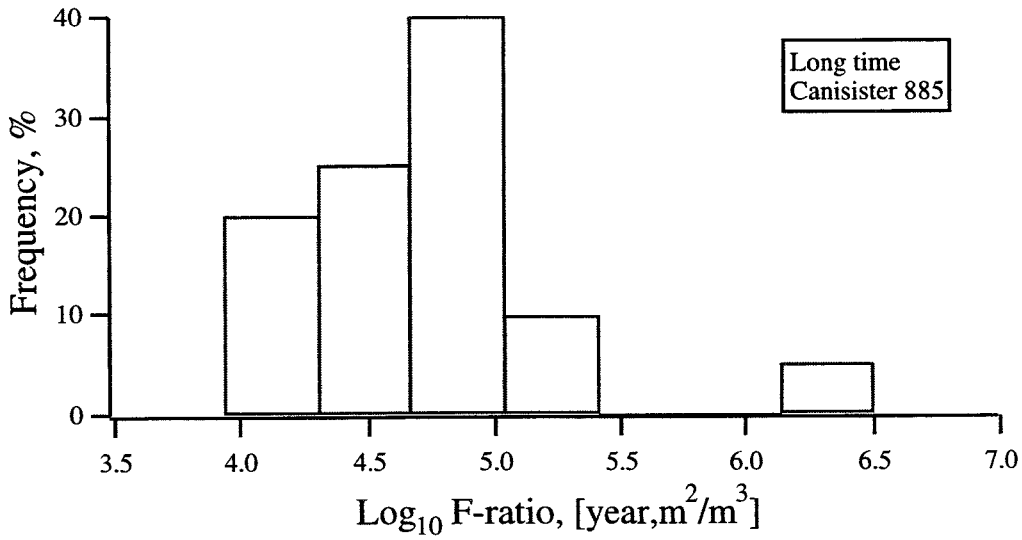

Figure 31. Histogram of F-ratio for canister 885.

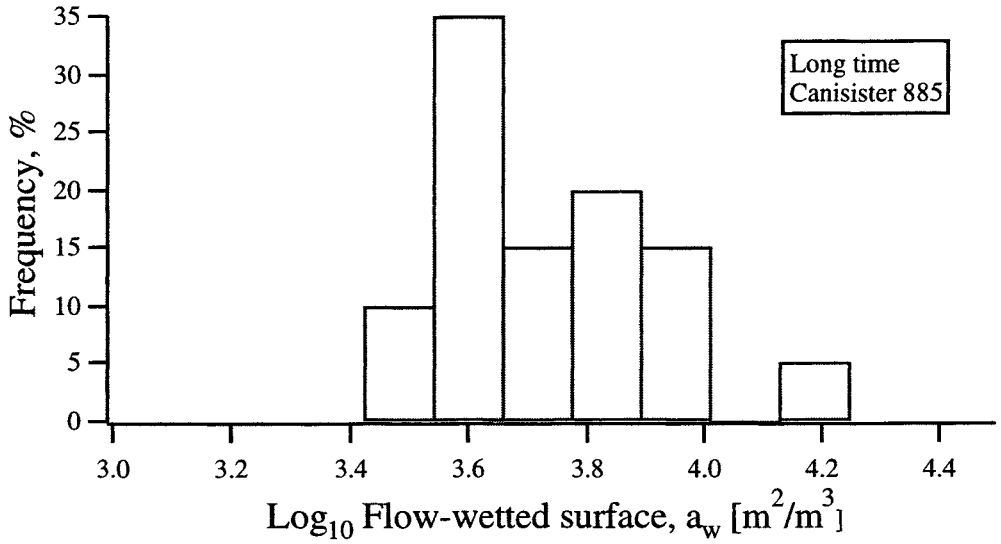

Figure 32. Histogram of flow-wetted surface based on volume of water for canister 885.

5.5 Performance measures by averaging over all realisations

Performance measures are calculated for all the entities, i.e. a measurement of the variation over all the realisations. The median and spread of medians for all entities y are reported. The mean of $\bar{y}$ and the variance of $\bar{y}$ are calculated, where $\bar{y}$ is the mean of the entities. A way to express these variations is by means of σ^2_y and the variance of σ^2_y where $y = \log_{10}(x)$. The variable x represents the Darcy velocity q, the travel time t, the F-ratio F, or the flow-wetted surface a_w. Performance measures may be also expressed as the median of the spread (dispersion) in results, MD_y and the spread in D_y defined as $UD_y = (D_y)_{95\%} - (D_y)_{5\%}$. Table 15 shows the performance measures for all the entities, using the different alternatives.

Table 15. Performance measures expressed as the median and spread of medians; y_{50}, mean and variance of $\bar{y}$, and the mean of σ^2_y, VAR[σ^2_y], median of the dispersion (MD_y) and the spread of the dispersion (UD_y).

	Darcy velocity fractures	T-water	F-ratio	a_w
Median (y_{50})	-3.269	1.035	4.873	3.759
Spread (y_{50})	0.123	0.084	0.103	0.040
Mean($\bar{y}$)	-3.133	1.025	4.831	3.800
VAR($\bar{y}$)	1.00E-03	4.40E-04	5.89E-04	1.04E-04
Mean(σ^2_y)	0.469	0.194	0.217	0.039
VAR[σ^2_y]	1.09E-03	3.89E-04	7.71E-04	1.41E-05
MD_y	2.375	1.449	1.494	0.593
UD_y	0.338	0.159	0.314	0.091

From the averages over all the realisations it can be concluded that the results seem to reach a Monte Carlo stability at the number of performed realisations. The presence of fracture zones has the dominating influence on the flow and transport in the rock. However, for a single canister the result may be very different between realisations. In some realisations there may be a fast path to a fracture zone whereas in other realisations the opposite may be valid. This effect may be smoothed out by first, averaging over all canisters and then, averaging over all realisations. The performance measures are shown in histograms in Figures 33 to 41.

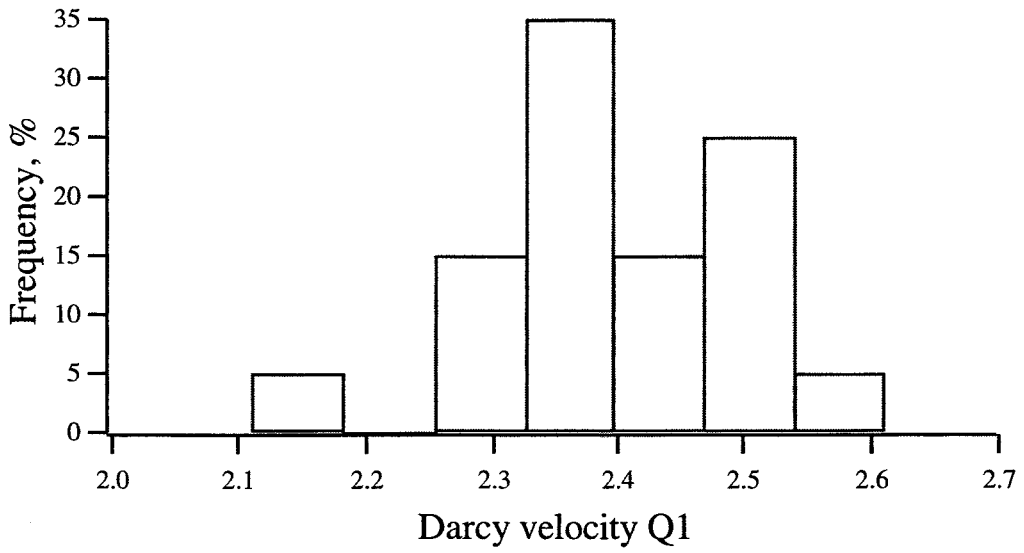

Figure 33. Dispersion, D_y, in Darcy velocity around the canister deposition hole.

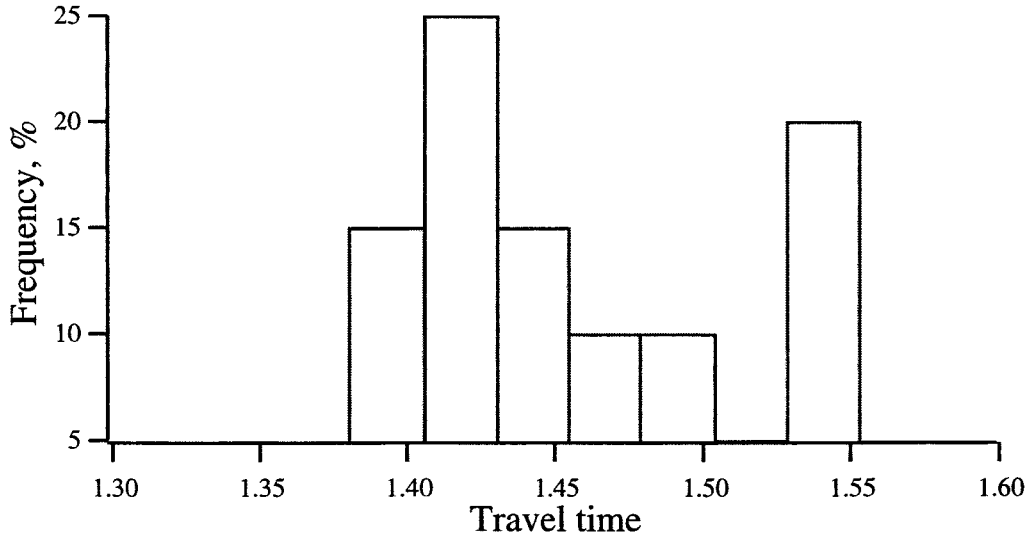

Figure 34. Dispersion, D_y, in travel time for the flow paths.

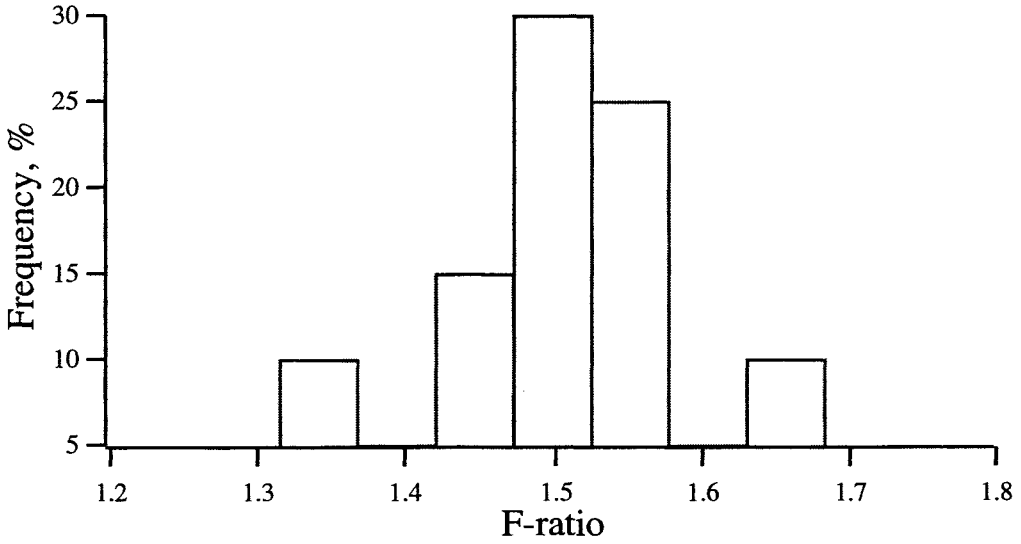

Figure 35. Dispersion, D_y, in F-ratio for the flow paths.

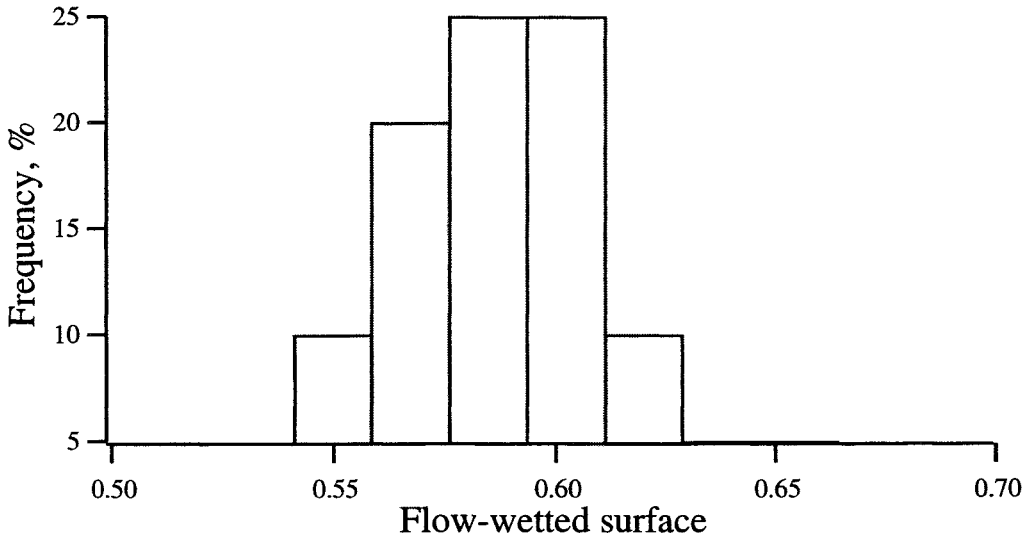

Figure 36. Dispersion, D_y, in flow-wetted surface for the flow paths.

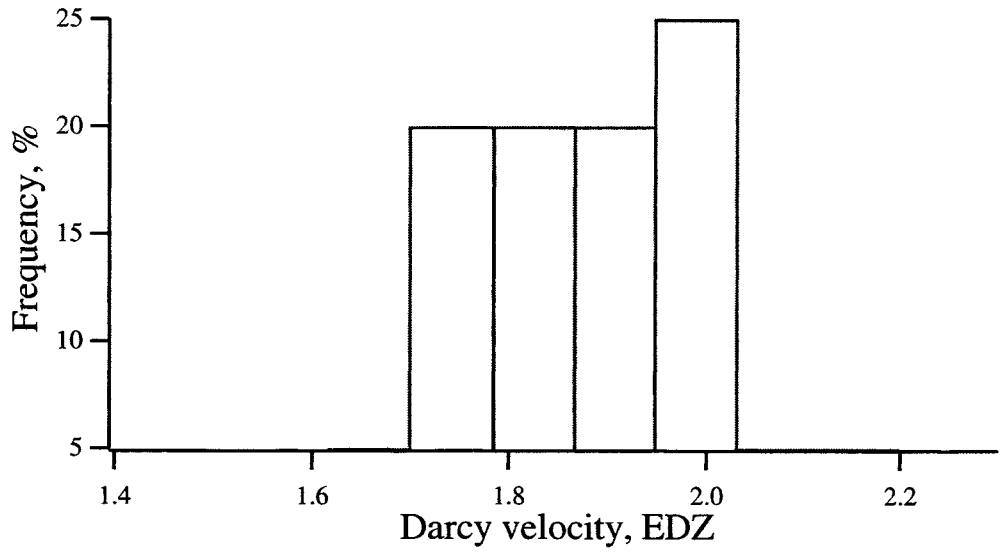

Figure 37. Dispersion, D_y, in Darcy velocity in the excavated disturbed zone.

Histograms of mean(y)

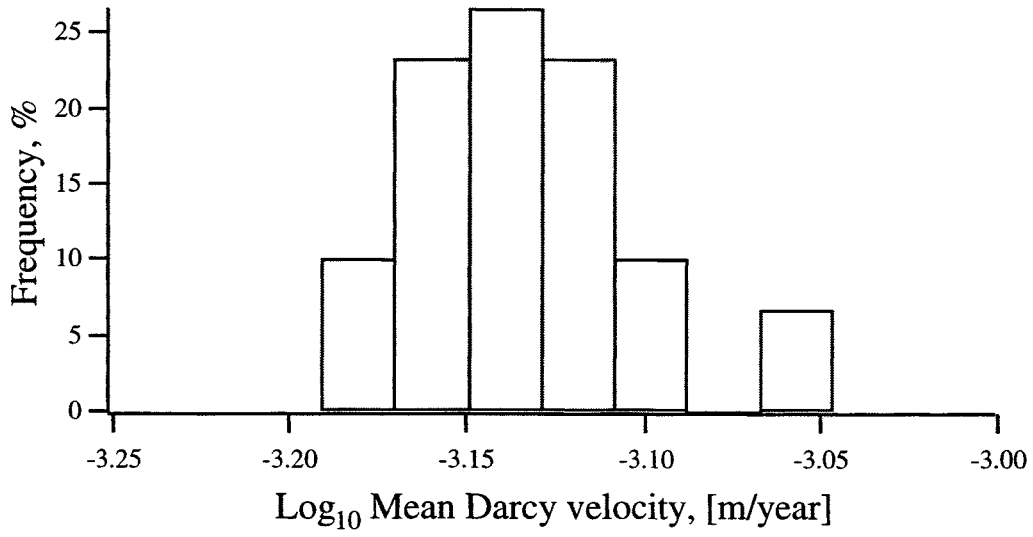

Figure 38. Mean Darcy velocity in the fractures in the repository domain.

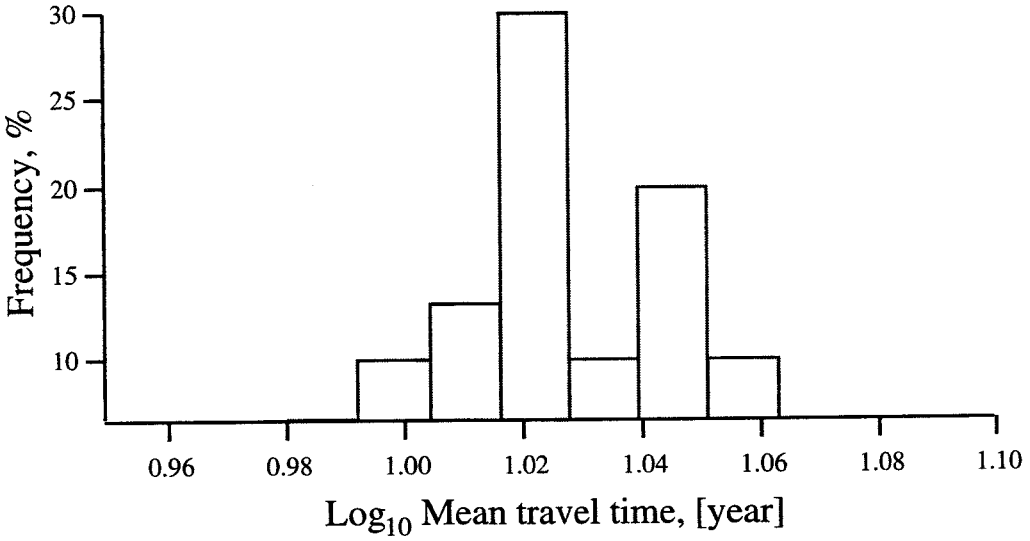

Figure 39. Mean travel time for the flow paths.

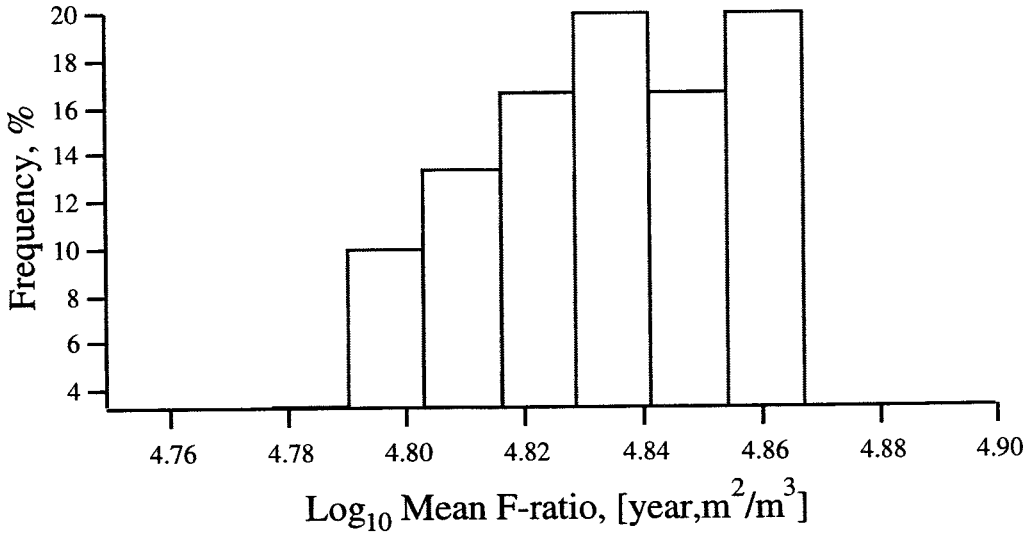

Figure 40. Mean F-ratio for the flow paths.

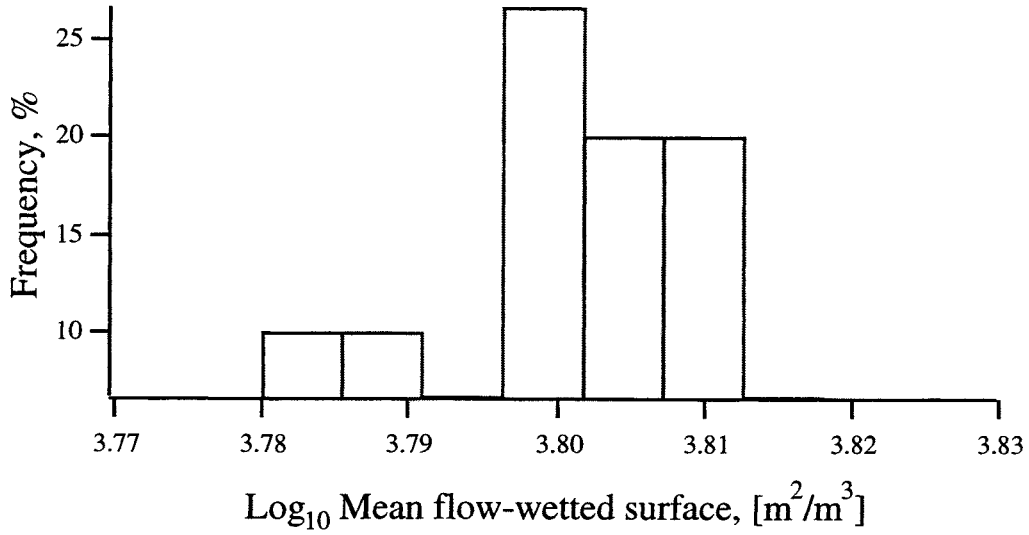

Figure 41. Mean flow-wetted surface for the flow paths.

5.6 Boundary flow consistency with the regional model

The net flows over the boundaries were calculated from the submitted boundary conditions of the regional simulations using PHOENIX (Svensson, 1997) and compared to one typical realisation using CHAN3D. To calculate the flow for the regional model the flux values were used. The comparison is shown in Table 16. Negative values mean net flow out from the system.

Table 16. Comparison of the net flow over the boundaries for the regional calculations and one realisation of CHAN3D.

Boundary	Regional net flow	CHAN3D net flow	Regional/CHAN3D
	[m^3/year]	[m^3/year]	
North	-3.06E+04	-5.86E+04	0.52
South	1.40E+04	5.81E+04	0.24
West	3.25E+05	3.80E+05	0.86
East	-1.12E+04	-2.32E+04	0.48
Top	-3.36E+05	-3.92E+05	0.86
Bottom	3.85E+04	3.55E+04	1.09

6 SUMMARY

In this study CHAN3D has been used to simulate production of input data to COMP23 and FARF31. CHAN3D has been integrated with COMP23 in earlier studies, but it has not been used before to calculate input data to FARF31. In the normal use of CHAN3D, the transport part of the concept simulates far field migration. The task in this study was to produce input data according a specification and using a defined hypothetical repository located at Äspö HRL as a platform. During the process of applying CHAN3D to the site, the scaling of conductivity was studied, using both data from Äspö HRL and synthetic data.

From the realisations performed, ensemble statistics of water travel time, flux at repository scale, flow-wetted surface and F-ratio values were calculated. Two typical realisations were studied in more detail. The results for three specified canister positions were also highlighted. Exit locations for the released particles were studied.

In each realisation statistics were calculated over the entities. The values were post-processed to obtain performance measures of higher order. From the averaging over all the realisations it can be concluded that the Monte Carlo stability is reached for the ensemble statistics. The presence of fracture zones has a large influence on flow and transport in the rock. However, for a single canister the result may be very different between realisations. In some realisations there may be a fast path to a fracture zone whereas in other realisations the opposite may be valid.

From the calculation of the flow over the boundaries between the regional model and the smaller local model the consistency seem to be acceptable considering that a perfect match of properties is hard to obtain.

REFERENCES

Andersson, J., M. Elert, L. Moreno, B. Gylling and J.O. Selroos, Derivation and treatment of the flow-wetted surface and other geosphere parameters in the models FARF31 and COMP23 for use in the safety assessment, SKB R-98-60, 1998.

Birgersson L., Widén H., Ågren T., Neretnieks I. Tracer migration experiment in the Stripa Mine 1980-1991. Stripa Project Technical Report 92-25, SKB, May 1992.

Gylling, B., L. Moreno, and I. Neretnieks, Simulation of radionuclide release from a repository to the biosphere. - Using a model coupling concept, Nuclear Technology, Vol. 122, 93-103, 1998a.

Gylling B., Moreno L., Neretnieks I., and Birgersson L., Analysis of a long-term pumping and tracer test using the Channel Network model, Journal of Contaminant Hydrology, Vol. 32, 203-222, 1998b.

Marsily, G. de, Hydrogeological parameters estimation techniques: Local test, model fitting, stochastic methods, and use of tracers, In Workshop on Appropriate Methodologies for Development and Management of Groundwater Resources in Developing Countries, Natl. Geophys. Res. Inst., India, 1989.

Moreno L., Tsang Y.W., Tsang C.F., Hale F.V., Neretnieks I. Flow and tracer transport in a single fracture. A stochastic model and its relation to some field observations, Water Resour. Res., 24, pp 2033-3048, 1988.

Moreno, L., B. Gylling, and I. Neretnieks, Solute transport in fractured media - the important mechanisms for performance assessment, Journal of Contaminant Hydrology, 25, 283-298, 1997.

Moridis, G. Personal communication. Lawrence Berkeley Laboratory, Berkeley, 1992.

Rhén I., G. Gustafson, R. Stanfors, and P. Wikberg, Äspö HRL - Geoscientific evaluation 1997/5, Models based on site characterization 1986-1995, SKB TR 97-06, 1997.

Romero L., L. Moreno, and I. Neretnieks, Fast multiple-path model to calculate radionuclide release from the near filed of a repository, Nuclear Technology, 112 (1), 89-98, 1995.

Romero L., L. Moreno, and I. Neretnieks, The fast multiple-path Nuctran model - Calculating the radionuclide release from a repository, Nuclear Technology, 112 (1) 99-107, 1995.

Sandstedt, H., R. Munier and L. Niland, Jämförelse av tentativa layouter, draft report, 1997-04-04, Scandiaconsult, Stockholm (In Swedish), 1997.

Ström A. "Data delivery 1", April 28 1997a.

Ström A. "Data delivery 2", May 15 1997b.

Ström A. and Selroos J-O. Use of alternative model for describing flow and transport in the far field, SKB PM May 16, 1997.

Svensson, U., A regional analysis of groundwater flow and salinity distribution in the Äspö area, SKB Technical Report 97-09, 1997.

APPENDIX

CONDENSED MODEL DESCRIPTION

Code:	CHAN3D
Model:	Channel Network model.
Code language:	The code is written in FORTRAN 77.
Origin of the code:	The code is developed by Luis Moreno, Ivars Neretnieks and Björn Gylling, Department of Chemical Engineering and Technology, Royal Institute of Technology, Stockholm.

General description

CHAN3D is a three-dimensional stochastic model based on the assumption that fluid flow and solute transport take place in a network of channels. In the model it is possible to include objects like fracture zones, boreholes and tunnels in a simplified manner. The dispersion caused by differences in solute pathway properties, like channel flow velocity, is inherently built into the model due to the stochastic generation of channel conductances. It is also possible to include solute and rock mass interaction processes, like sorption and diffusion into the rock matrix, in the simulations.

Conceptual and Mathematical model

Each member of the network is assigned a hydraulic conductance. This is the only entity needed to calculate the flow, if the pressure field is known. The conductance is defined as the ratio between the flow in a channel and the pressure difference between its ends. The pressure field is calculated by writing the mass balance at each channel intersection point. If the residence time for non-interacting solutes is to be calculated, then the volume of the channel members is needed as well. If sorption onto the fracture surface or diffusion into the matrix will be included in the model, the surface area of the flow-wetted surface and rock properties must also be included.

Here, the conductances of the channel members are assumed to be log-normally distributed, with mean μ_C and standard deviation σ_C. Different values are used for the mean conductance depending on where the channel members are located.

Numerical method

The large system of equations which are obtained are solved by a solver which uses the preconditioned gradient method (Moridis, personal communication, 1992). Some standard routines such as RANDOM and SORT are also used. For the tracer test simulation a particle-following method is used (Moreno et al., 1988).

Parameters required

- The distribution of conductances (the channel length is included in this entity).
- For non-interacting solutes the channel volumes or the flow porosity must be known.
- For the interacting solutes the flow-wetted surface is an important entity.
- Properties of the rock are needed as well, such as rock matrix porosity, diffusivity, and sorption capacity for sorbing species.
- Geometric information for objects like fracture zones and tunnels.
- Boundary conditions.

Type of results

The results can be obtained as head or pressure field, flow field and breakthrough curves for step or pulse injection. In the present AMP project the code has been extended to calculate the requested input entities.

Computer requirements

Any computer, which may handle a FORTRAN 77 code and has a sufficiently large memory, can be used. The memory requirement is quite large if the number of channels is large. For example,

in the simulations of LPT2 we used about 66 000 nodes or channel intersections. We have then used the memory required for storing about ten million real double precision variables and ten million integer variables.

Model application

The Channel Network model is developed as a tool in the performance assessment of a potential site for storage of hazardous waste at depth in crystalline rock and general studies of flow and transport in fractured rock. The model is flexible in the sense that it is easy to incorporate geometric information from a site and boundary conditions can easily be varied.

The model has been used to simulate the performed experiments at the Stripa site (Birgersson et al., 1992), the conditions at the SFR repository, and the analysis of the field experiments, LPT2 and TRUE, experimentally carried out at Äspö Hard Rock Laboratory (Gylling et al., 1998a). It has also been used in performance assessment calculations for tentative repository layouts.

Condensed model descriptions, using the LPT2 study as an example, is shown in Table A1 and A2. Table A1 shows the model concept used in the hydraulic study and Table A2 shows the concept for the tracer test simulations. In these tables the concepts, input data and boundary conditions used are displayed together with the types of output results available.

Table A1. Condensed conceptual model description of the Channel Network model used for simulations of drawdown in the LPT2 experiment carried out at Äspö HRL.

SIMULATION MODEL FOR THE LPT2 DRAWDOWN TEST Channel network model	
Process description Equation of continuity (flow balances) Equation of motion (flow driven by head gradient)	
CONCEPTS	DATA
Geometric framework and parameters	
3D box divided into:	Size: 1.0x0.7x0.7 km
3D fracture zones (planar with a thickness), some with limited extent	Zone geometry, location and extent from geological structural model
Standard deviation in K	Hydraulic packer tests
Material properties	
Zones: Channel conductivity K	Transmissivity data
Rock mass: Channel conductivity K	K from rock mass measurements
Spatial assignment method	
Channels within fracture zones, K from log-normal distribution with mean $K(T_i)$	Zone geometry, location and extent from geological structural model
Channels within rock mass K from log-normal distribution with mean K(rock mass)	
Boundary conditions	
Upper: Infiltration	Infiltration based on precipitation and assumptions about run-off and evaporation
Lower: No flow	
Sides: Constant head	
Withdrawal borehole: Inflow or drawdown	Inflow and drawdown data
Numerical tool Channel Network model	
Output parameters Hydraulic head and flow-rate distribution	

Table A2. Condensed conceptual model description of the Channel Network model used for simulations of tracer tests in the LPT2 experiment carried out at Äspö HRL.

SIMULATION MODEL FOR THE LPT2 TRACER TESTS Channel network model	
Process description Mass balance (advection, matrix diffusion and dispersion)	
CONCEPTS	DATA
Geometric framework and parameters	
3D box divided into: 3D fracture zones (planar with a thickness), some with limited extent	Size: 1.0x0.7x0.7 km Zone geometry, location and extent from geological structural model
Material properties	
Flow distribution Flow-wetted surface Diffusion coefficient Sorption capacity Flow porosity	From drawdown simulation, CHAN3D-flow Hydraulic packer tests Estimated based on data from other sites Non-sorbing tracers used Unknown, parameter variation tested
Spatial assignment method	
Locations for injections and detection Dispersion due to heterogeneous flow field	Injection and detection location data, borehole data and zone geometry Flow distribution from drawdown simulation with CHAN3D-flow
Boundary conditions	
Injection: Temporal injection	Injection data
Numerical tool Channel Network model and particle following algorithm	
Output parameters Residence time distribution, breakthrough curves and particle trace	